

Rhodium(III) and Rhodium(II) Complexes of Novel Bis(oxazoline) Pincer Ligands

Michael Gerisch, Jennifer R. Krumper, Robert G. Bergman,* and T. Don Tilley*

Department of Chemistry and Center for New Directions in Organic Synthesis (CNDOS),
University of California and Division of Chemical Sciences, Lawrence Berkeley
National Laboratory, Berkeley, California 94702

Received September 11, 2002

A series of novel C_2 -symmetric bisoxazoline ligands (benbox and benboxMe₂) have been prepared. A variety of coordinatively unsaturated rhodium(III) complexes (**3a–g**, **4a–g**) have been isolated. Trapping reactions of the agostically stabilized complex [RhCl₂{(S,S)-ib-benbox(Me₂)}] (**4d**) are described. Metal-to-aryl methyl migration reactions are described for the complex [RhMe{(S,S)-ip-benbox(Me₂)}][BAR_f] (**11c**). Full characterization details and reactivity studies of air-stable, isolable, mononuclear, paramagnetic rhodium(II) complexes [RhCl₂{(S,S)-tb-benbox(Me₂)}(H)] (**15e**) and [RhCl₂{dm-benbox(Me₂)H}] (**15g**) are reported.

Introduction

C_2 -symmetric bisoxazoline ligands are easily prepared from commercially available chiral starting materials, and their metal complexes display remarkable efficacy in a wide variety of important organic transformations.¹ In one example, Nishiyama and co-workers prepared a variety of metal complexes of the trischelating C_2 -symmetric bisoxazoline ligand 2,6-bis(2-oxazolin-2-yl)pyridine (pybox).² Pybox ligand complexes have proven to be effective catalysts for a variety of enantioselective transformations, including hydrosilylation of ketones^{2b} and cyclopropanation of olefins.³ However, these processes are somewhat limited by the lability of the datively bound pybox ligand, which may result in low enantiomeric excesses and makes these catalysts unsuitable for applications at elevated temperatures.^{2a,4}

Monoanionic tridentate ligands, such as the “PCP pincer” (alkyl or aryl bis(phosphino)) and “NCN pincer” (alkyl or aryl bis(amino)) ligands bind more tightly to metal centers than trischelate ligands that can form only dative bonds. Transition metal complexes of pincer ligands have been applied to carbon–carbon bond cleavage,⁵ catalytic aliphatic dehydrogenation,⁶ Kharasch reactions,⁷ methylene transfers,⁸ and various catalytic enantioselective transformations.⁹ Pincer ligand complexes are quite thermally robust, presumably due to the strong covalent bond between a monoanionic tridentate ligand and the metal center.

In recent years, NCN pincer ligands that resemble pybox have been prepared.¹⁰ The metal complexes of these 2,6-bis(oxazoly)phenyl (phebox) ligands have been used as catalysts for the enantioselective allylation of aldehydes,¹¹ Diels–Alder reactions,^{10b} alkylation of aldimines,¹² and cyclopropanation.^{10c} The C_2 -symmetric phebox ligands feature the ease of preparation and chirality of pybox, as well as the robust binding motif found in pincer ligands.

We are interested in developing new C_2 -symmetric pincer ligands for use in metal-catalyzed enantioselective transformations. Our ligand design was guided by preliminary molecular mechanics modeling, which suggested that benzylic homologation of phebox would widen the ligand N–M–N bite angle. Bite angle has been shown to have a dramatic effect on the reactivity of a variety of metal–ligand complexes.¹³ Bite angle controls the steric environment around the metal center and also directly affects the shape and energy of the metal frontier molecular orbitals. Additionally, our preliminary molecular mechanics models predicted that

(6) (a) Liu, F. C.; Pak, E. B.; Singh, B.; Jensen, C. M.; Goldman, A. S. *J. Am. Chem. Soc.* **1999**, *121*, 4086. (b) Jensen, C. M. *Chem Commun.* **1999**, 2443. (c) Lee, D. W.; Kaska, W. C.; Jensen, C. M. *Organometallics* **1998**, *17*, 1. (d) Gupta, M.; Hagen, C.; Kaska, W. C.; Cramer, R. E.; Jensen, C. M. *J. Am. Chem. Soc.* **1997**, *119*, 840. (e) Gupta, M.; Kaska, W. C.; Jensen, C. M. *Chem. Commun.* **1997**, 461. (f) Gupta, M.; Hagen, C.; Flesher, R. J.; Kaska, W. C.; Jensen, C. M. *Chem. Commun.* **1996**, 2083.

(7) (a) van de Kuil, L. A.; Grove, D. M.; Gossage, R. A.; Zwikker, J. W.; Jenneskens, L. W.; Drenth, W.; van Koten, G. *Organometallics* **1997**, *16*, 4985. (b) Gossage, R. A.; van de Kuil, L. A.; van Koten, G. *Acc. Chem. Res.* **1998**, *31*, 423.

(8) Gozin, M.; Aizenberg, M.; Liou, S. Y.; Weisman, A.; Ben-David, Y.; Milstein, D. *Nature* **1994**, 42.

(9) For examples, see: (a) Seligson, A. L.; Trogler, W. C. *Organometallics* **1993**, *12*, 744. (b) Gorla, F.; Venanzi, L. M. *Organometallics* **1994**, *13*, 43. (c) Ohff, A.; Ohff, M.; Milstein, D. *J. Am. Chem. Soc.* **1997**, *119*, 11687.

(10) (a) Motoyama, Y.; Makihara, N.; Mikami, Y.; Aoki, K.; Nishiyama, H. *Chem. Lett.* **1997**, 951. (b) Stark, M. A.; Richards, C. J. *Tetrahedron Lett.* **1997**, *38*, 5881. (c) Denmark, S. E.; Stavanger, R. A.; Faucher, A. M.; Edwards, J. P. *J. Org. Chem.* **1997**, *62*, 3375.

(11) Motoyama, Y.; Narusawa, H.; Nishiyama, H. *Chem. Commun.* **1999**, 131.

(12) Motoyama, Y.; Mikami, Y.; Kawakami, H.; Aoki, K.; Nishiyama, H. *Organometallics* **1999**, *18*, 3584.

* To whom correspondence should be addressed. E-mail: bergman@chem.berkeley.edu (R.G.B.); tdtiley@socrates.berkeley.edu (T.D.T.).

(1) For reviews, see: (a) Pfaltz, A. *Acc. Chem. Res.* **1993**, *26*, 339. (b) Ghosh, A. K.; Mathivanan, P.; Cappiello, J. *Tetrahedron: Asymmetry* **1998**, *9*, 1. (c) Ojima, I. *Catalytic Asymmetric Synthesis*, 2nd ed.; Wiley-VCH: New York, 2000. (d) Fache, F.; Schulz, E.; Tommasino, M. L.; Lemaire, M. *Chem. Rev.* **2000**, *100*, 2159.

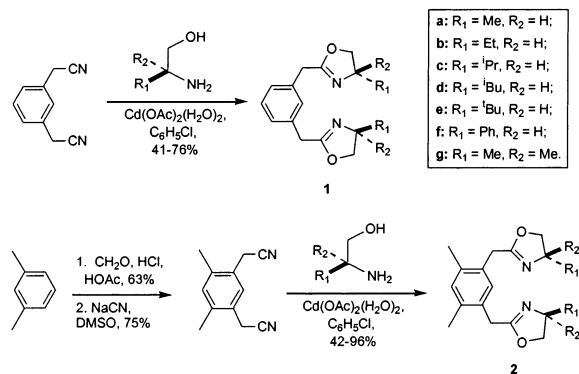
(2) (a) Nishiyama, H.; Sakaguchi, H.; Nakamura, T.; Horihata, M.; Kondo, M.; Itoh, K. *Organometallics* **1989**, *8*, 846. (b) Nishiyama, H.; Kondo, M.; Nakamura, T.; Itoh, K. *Organometallics* **1991**, *10*, 500.

(3) Nishiyama, H.; Itoh, Y.; Matsumoto, H.; Park, B.; Itoh, K. *J. Am. Chem. Soc.* **1994**, *116*, 2223.

(4) Nesper, R.; Pregosin, P. S.; Püntener, K.; Wörle, M.; Albinati, A. *J. Organomet. Chem.* **1996**, *507*, 85.

(5) Rybtchinski, B.; Milstein, D. *Angew. Chem., Int. Ed. Engl.* **1999**, *38*, 871.

Scheme 1. Ligand Synthesis



widening the N–M–N bite angles of phebox-type complexes would draw the oxazolyl alkyl groups closer to the metal center than previously observed. The resulting complexes should possess a more sterically congested ligand environment, which might, in turn, lead to higher selectivities in catalysis.

We prepared two series of new NCN pincer ligands, the parent bis(oxazolylmethyl)benzene ((*S,S*)-benbox) ligands **1a–g** and the methylated (*S,S*)-bis(oxazolylmethyl)-4,6-dimethylbenzene ((*S,S*)-benboxMe₂) ligands **2a–g** (Scheme 1), which were expected to resist metalation in the 4- and 6-positions of the aromatic ring.¹⁴ We have recently reported the synthesis of monomeric rhodium(II) and coordinatively unsaturated rhodium(III) metal complexes of the benbox and benboxMe₂ ligands.¹⁵ In this report we fully describe the synthesis and reaction chemistry of these complexes.

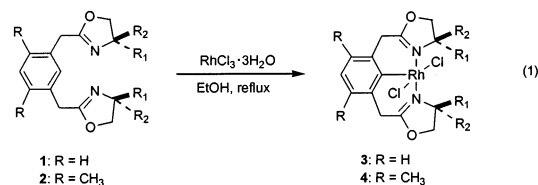
Results and Discussion

Ligand Synthesis. All amino alcohols employed in the ligand syntheses are commercially available as both enantiomers (with the exception of *tert*-leucinol, which is only available as the (*S*) antipode), as is the dinitrile used in the synthesis of ligands **1a–g**. The *meta*-dimethyl dinitrile (for ligands **2a–g**) was synthesized from 2,4-dimethyldi-1,5-(chloromethyl)benzene, which was obtained by chloromethylation of *m*-xylene.^{16,17} The new benbox and benboxMe₂ ligands **1a–g** and **2a–g** were obtained using the procedure reported by Witte and Bolm for the synthesis of the corresponding phebox ligands (Scheme 1).¹⁸ Each benbox ligand was prepared by refluxing a solution of the appropriate dinitrile with an excess of the appropriate amino alcohol in chloroben-

zene in the presence of catalytic Cd(OAc)₂·2H₂O. Column chromatography was used to purify the ligands, which were obtained in good to moderate yields as white or yellow solids (melting points = 56–86 °C) and were fully characterized. Enantiomerically pure bis(oxazolines) were additionally characterized by optical rotation.

Several methods of spectroscopic characterization were used to establish the C₂-symmetry of ligands **1a–g** and **2a–g**. Only one C–N stretching vibration appears in the IR spectra of these ligands, in the range 1659–1670 cm⁻¹. The ¹H NMR spectra of the ligands are also consistent with a C₂-symmetrical environment; a doublet of doublet splitting for the oxazoline CH₂'s is observed. The oxazolyl-carbon atom resonances in the ¹³C{¹H} NMR spectra were observed between 163.3 and 167.0 ppm.

Synthesis of Rhodium(III) Complexes. Syntheses of the rhodium(III) benbox and benboxMe₂ complexes were based on previously reported procedures for cyclometalated rhodium pincer ligand compounds.^{10a,19} Addition of RhCl₃·3H₂O to refluxing ethanolic solutions of **1a–g** or **2a–g** led in all cases to formation of the corresponding rhodium(III) complexes [RhCl₂(benbox)] (**3a–g**) and [RhCl₂(benboxMe₂)] (**4a–g**) in 8–59% yield (eq 1). In contrast to related 18-valence-electron “NCN



pincer” rhodium(III) complexes, which were obtained as H₂O adducts, the benbox and benboxMe₂ complexes are coordinatively unsaturated.^{10a,19b} This effect is presumably a result of steric shielding of the open coordination site by the pincer ligand (vide infra).

Rhodium(III) benbox and benboxMe₂ complexes **3a–g** and **4a–g** were isolated as orange, air-stable microcrystalline compounds which are highly soluble in methylene chloride and tetrahydrofuran and moderately soluble in benzene and acetone. Coordination of the bis(oxazoline) ligand to the metal center results (except in the case of **3e**) in an increase in the frequency for the C–N stretching vibration relative to those of the free ligand, giving rise to ν_{CN} values between 1668 and 1683 cm⁻¹. These results differ from those reported for the (phebox)-rhodium(III) complexes, in which a decrease of the frequency is observed upon coordination.^{10a} This difference may be related to a bite-angle-induced change in the metal–ligand orbital overlap.

The two hydrogens attached to each bridging methylene carbon are diastereotopic in all rhodium(III) complexes of benbox and benboxMe₂ ligands containing a stereogenic center and give rise to two doublets in the ¹H NMR spectra between 5.25 and 3.28 ppm (*J*_{HH} = 16.8–19.0 Hz). The resonances due to the metal-bound *ipso*-carbons in **3a–g** and **4a–g** appear between 129.5 and 135.5 ppm in the ¹³C{¹H} spectrum, revealing

(13) (a) Casey, C. P.; Whiteker, G. T. *Isr. J. Chem.* **1990**, *30*, 299. (b) Casey, C. P.; Whiteker, G. T.; Melville, M. G.; Petrovich, L. M.; Gavney, J. A.; Powell, D. R. *J. Am. Chem. Soc.* **1992**, *114*, 5535. (c) Hansen, S. M.; Rominger, F.; Metz, M.; Hofmann, P. *Chem.-Eur. J.* **1999**, *5*, 557. (d) van Leeuwen, P.; Kamer, P. C. J.; Reek, J. N. H.; Dierkes, P. *Chem. Rev.* **2000**, *100*, 2741. (e) Kamer, P. C. J.; van Leeuwen, P. W. N.; Reek, J. N. H. *Acc. Chem. Res.* **2001**, *34*, 895.

(14) (a) Steenwinkel, P.; James, S. L.; Grove, D. M.; Kooijman, H.; Spek, A. L.; van Koten, G. *Organometallics* **1997**, *16*, 513. (b) Steenwinkel, P.; James, S. L.; Gossage, R. A.; Grove, D. M.; Kooijman, H.; Smeets, W. J. J.; Spek, A. L.; van Koten, G. *Organometallics* **1998**, *17*, 4680. (c) Steel, P. J.; Hartshorn, C. M. *Organometallics* **1998**, *17*, 3487.

(15) Gerisch, M.; Krumper, J. R.; Bergman, R. G.; Tilley, T. D. *J. Am. Chem. Soc.* **2001**, *123*, 5818.

(16) van der Made, A. W.; van der Made, R. H. *J. Org. Chem.* **1993**, *58*, 1262.

(17) Ciba Corp. Patent, US 3483209, 1969.

(18) (a) Bolm, C.; Weickhardt, K.; Zehnder, M.; Rauff, T. *Chem. Ber.* **1991**, *124*, 1173. (b) Witte, H.; Seeliger, W. *Liebigs Ann. Chem.* **1976**, *996*.

(19) (a) Moulton, C. J.; Shaw, B. L. *J. Chem. Soc., Dalton Trans.* **1976**, 1020. (b) van der Zeijden, A. A. H.; van Koten, G.; Luijk, R.; Vrieze, K.; Slob, C.; Krabbendam, H.; Spek, A. L. *Inorg. Chem.* **1988**, *27*, 1014.

Table 1. Crystal Data and Structure Refinement for 4c, 9c, and 15g

| | 4c | 9c | 15g |
|--|--|---|---|
| Crystal Data | | | |
| empirical formula | C ₂₂ H ₃₁ Cl ₂ N ₂ O ₂ Rh·CH ₂ Cl ₂ | C ₂₂ H ₃₀ F ₃ N ₂ O ₅ SRh | C ₂₀ H ₂₈ Cl ₂ N ₂ O ₂ Rh |
| fw | 614.24 | 594.45 | 502.27 |
| cryst color, habit | orange, columnar | yellow, blade | orange, dendritic |
| cryst dimens (mm) | 0.33 × 0.12 × 0.12 | 0.30 × 0.17 × 0.02 | 0.15 × 0.20 × 0.30 |
| cryst syst | orthorhombic | monoclinic | monoclinic |
| lattice type | primitive | primitive | primitive |
| lattice params | <i>a</i> = 8.3012(2) Å <i>b</i> = 16.1358(4) Å <i>c</i> = 19.2670(5) Å | <i>a</i> = 9.4600(3) Å <i>b</i> = 53.891(2) Å <i>c</i> = 9.7688(3) Å <i>β</i> = 92.453(1)° | <i>a</i> = 9.0415(4) Å <i>b</i> = 12.3993(5) Å <i>c</i> = 10.0072(4) Å <i>β</i> = 95.135(1)° |
| <i>V</i> (Å ³) | 2580.75(10) | 4975.7(3) | 1117.39(8) |
| space group | <i>P</i> 2 ₁ 2 ₁ 2 ₁ (#19) | <i>P</i> 2 ₁ (#4) | <i>P</i> 2 ₁ (#4) |
| <i>Z</i> value | 4 | 8 | 2 |
| <i>D</i> _{calc} (g/cm ³) | 1.581 | 1.587 | 1.493 |
| <i>F</i> ₀₀₀ | 1256.00 | 2432.00 | 514.00 |
| <i>μ</i> (Mo Kα) (cm ⁻¹) | 10.97 | 8.26 | 10.18 |
| Intensity Measurements | | | |
| temperature (°C) | -127 ± 1 | -102 ± 1 | -102 ± 1 |
| 2θ range (deg) | 3.00–46.00 | 3.50–45.00 | 3.00–45.00 |
| 2θ _{max} (deg) | 52.1 | 46.6 | 52.0 |
| no. of reflns measd | total: 12 541 unique: 2725 (<i>R</i> _{int} = 0.035) | total: 21 101 unique: 7428 (<i>R</i> _{int} = 0.091) | total: 5412 unique: 2269 (<i>R</i> _{int} = 0.026) |
| Structure Solution and Refinement | | | |
| <i>p</i> -factor | 0.0300 | 0.0300 | 0.0300 |
| no. of observations (<i>I</i> > 3.00σ(<i>I</i>)) | 3686 | 6812 | 3022 |
| no. of variables | 289 | 749 | 239 |
| refln/param ratio | 12.75 | 9.09 | 12.64 |
| residuals: ^a <i>R</i> , <i>R</i> _w , <i>R</i> _{all} | 0.025, 0.026, 0.037 | 0.068, 0.068, 0.106 | 0.029, 0.044, 0.030 |
| goodness of fit indicator | 0.98 | 1.93 | 1.92 |
| max. shift/error in final cycle | 0.00 | 0.01 | 0.01 |

$$^a R = \sum ||F_o| - |F_c|| / \sum |F_o|, R_w = [\sum w(|F_o| - |F_c|)^2 / \sum w F_o^2]^{1/2}, \text{ where } w = 1/\sigma^2(F_o).$$

almost no change in chemical shift relative to the starting ligand, and an upfield shift of roughly 50 ppm compared to those in the (phebox)-rhodium(III) complexes reported by Nishiyama et al.^{10a} The ¹J_{Rh-C} coupling constants range from 34.5 to 39.4 Hz.

Orange crystals of **4c** suitable for X-ray analysis were obtained by layering a CH₂Cl₂ solution of **4c** with pentane at room temperature. The molecular structure is shown in Figure 1, crystal data and structure refinement information is presented in Table 1, and selected bond distances and angles are given in Table 2. The rhodium atom adopts a square pyramidal coordination environment, with the aryl ring of the pincer ligand in the apical position. The structural parameters for **4c** can be compared to those of the related five-membered chelate complex [RhCl₂(*t*-BuNC)((*S,S*)-ip-phebox)].^{10a} The six-membered metal–ligand chelate ring results in an N–Rh–N angle for **4c** (178.01(1)°) that is much larger than that in the phebox complex (157.3(2)°). Consequently, the ligand isopropyl groups are quite close to the metal center in complex **4c**. The Rh···C(21) (3.11 Å) and Rh···H(C(21)) (2.38 Å) distances and the Rh–H–C(21) angle (133.8°) are consistent with a weak Rh–H agostic interaction between the isopropyl group and rhodium. The Rh–C(9) distance of 2.004(3) Å is slightly longer than the corresponding value in the (phebox)-rhodium(III) complex (1.941(7) Å).^{10a} The Rh–Cl distances (2.355(2), 2.365(1) Å) are equivalent within 3σ, as are the Rh–N distances (2.074(4), 2.072(4) Å). The Rh–N bond lengths in the benbox complex are similar to those reported for the (phebox)-rhodium(III) complex (2.053(5), 2.055(5) Å).^{10a}

Although the X-ray structure of **4c** reveals a weak Rh–H interaction involving one isopropyl group and the

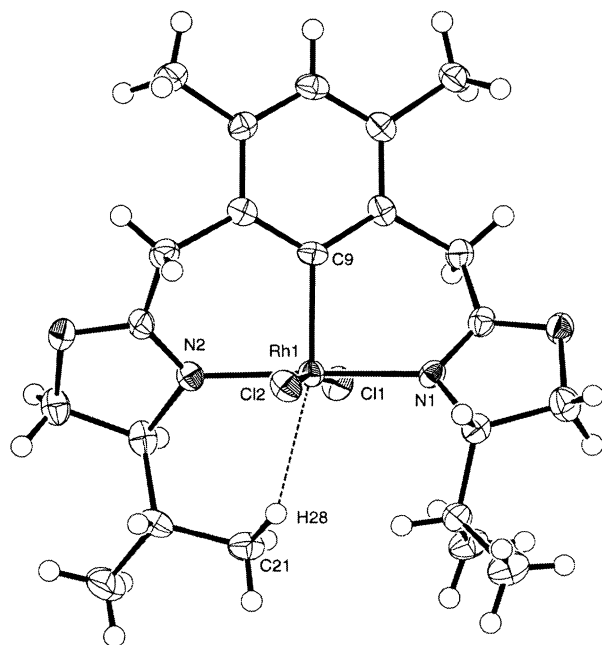
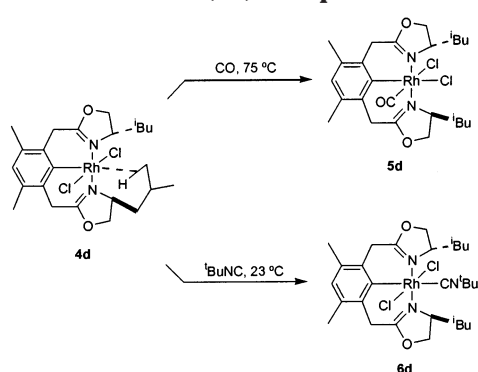


Figure 1. Molecular structure of **4c**. Methylene chloride molecule is omitted for clarity. Thermal ellipsoids are shown at the 50% probability level.

rhodium center, no IR band could be assigned to an agostic C–H vibration for this complex. However, the complexes **3d** and **4d**, bearing isobutyl substituents at the oxazoline rings, exhibit two low-frequency bands of medium strength (**3d**: $\nu_{\text{RhCH}} = 2762, 2752 \text{ cm}^{-1}$, **4d**: $\nu_{\text{RhCH}} = 2764, 2756 \text{ cm}^{-1}$) assigned to the agostic C–H

Table 2. Selected Distances (Å) and Bond Angles (deg) for [RhCl₂{(S,S)-ip-benboxMe₂}] (**4c**)

| | | | |
|-------------|----------|-------------------|----------|
| Rh(1)–Cl(1) | 2.336(1) | Cl(1)–Rh(1)–Cl(2) | 170.9(4) |
| Rh(1)–Cl(2) | 2.336(1) | N(1)–Rh(1)–N(2) | 178.0(1) |
| Rh(1)–N(1) | 2.032(3) | Cl(1)–Rh(1)–C(9) | 93.8(1) |
| Rh(1)–N(2) | 2.026(3) | Cl(2)–Rh(1)–C(9) | 95.3(1) |
| Rh(1)–C(9) | 2.004(3) | N(1)–Rh(1)–C(9) | 90.1(1) |
| Rh(1)⋯C(21) | 3.11 | N(2)–Rh(1)–C(9) | 91.5(1) |

Scheme 2. Trapping the Unsaturated Rhodium(III) Complexes

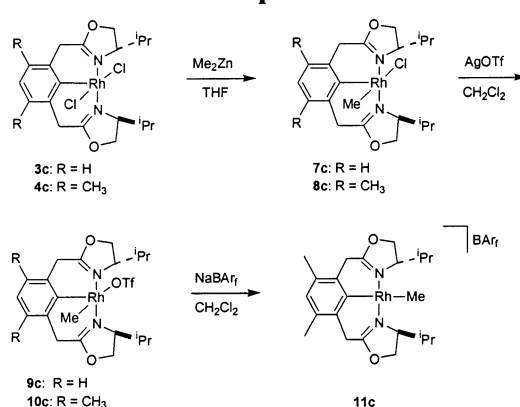
stretching frequencies.²⁰ No upfield resonances for these agostic interactions were observed in the ¹H NMR spectrum from room temperature to –88 °C.

Coordinatively Saturated Rhodium(III) Complexes. Reaction of **4d** with excess CO led to the formation of [RhCl₂{(S,S)-ip-benbox(Me₂)}(CO)] (**5d**) (90%) after 3 days at 75 °C (Scheme 2). Over the course of the reaction, the two IR bands assigned to the weak Rh–C–H interactions in **4d** disappeared and were replaced by a strong C–O stretching vibration at 2070 cm⁻¹. Furthermore, the C–N stretching vibration of the oxazoline ring was observed at a lower wavenumber ($\nu_{\text{CN}} = 1666 \text{ cm}^{-1}$) than that in **4d** ($\nu_{\text{CN}} = 1683 \text{ cm}^{-1}$). The appearance of four different resonances for the methyl protons of the isobutyl groups in the ¹H NMR spectrum of **5d** and the lack of chemically equivalent isobutyl carbon atoms in the ¹³C{¹H} NMR spectrum of this complex are indicative of a *cis*-arrangement of the chloride ligands.

Reaction of **4d** with *tert*-butylisocyanide at room temperature led to formation of [RhCl₂{(S,S)-ip-benbox(Me₂)}(^tBuNC)] (**6d**) (82%) within seconds (Scheme 2). As in the reaction with carbon monoxide, the two IR bands for the agostic interactions in **4d** disappeared and were replaced by a strong C–N stretching vibration at 2177 cm⁻¹ for the coordinated ^tBuNC in **6d**. As with carbonyl complex **5d**, the C–N stretching vibration of the oxazoline ring for **6d** ($\nu_{\text{CN}} = 1669 \text{ cm}^{-1}$) is observed at a lower wavenumber than that in **4d** ($\nu_{\text{CN}} = 1683 \text{ cm}^{-1}$). The ¹H NMR spectrum of **6d** is consistent with a C₂-symmetric molecule, implying a *trans* arrangement of the chloride ligands. The difference in stereochemistry between complexes **5d** and **6d** may be caused by the need for avoidance of unfavorable steric interactions between the oxazolyl alkyl groups and the isocyanide *tert*-butyl group in **6d**.

Synthesis and Reactivity of Methylrhodium(III)

(20) (a) Brookhart, M.; Green, M. L. H.; Wong, L. L. *Prog. Inorg. Chem.* **1988**, *36*, 1. (b) Crabtree, R.; Hamilton, D. G. *Adv. Organomet. Chem.* **1988**, *28*, 299.

Scheme 3. Synthesis of Methylrhodium Complexes

Complexes. Inspired by the results of Milstein et al.^{5,21} and van Koten et al.,²² we explored the synthesis and reactivity of methylrhodium(III) complexes bearing benbox ligands. Although treatment of the dichlororhodium(III) complex **3c** or **4c** with methyllithium or methyl Grignard reagents led to decomposition, dimethylzinc was found to be an effective methylating agent. When **3c** or **4c** was treated with dimethylzinc in tetrahydrofuran, a color change from orange to yellow was observed. After treatment with alumina(III), the methyl-(chloro)rhodium(III) complexes **7c** (37%) and **8c** (36%) were obtained (Scheme 3).

Little variation is observed when comparing the ligand C–N stretching vibrations of the dichlororhodium complexes **3c** ($\nu_{\text{CN}} = 1674 \text{ cm}^{-1}$) and **4c** ($\nu_{\text{CN}} = 1680 \text{ cm}^{-1}$) with those of the methylrhodium complexes **7c** ($\nu_{\text{CN}} = 1673 \text{ cm}^{-1}$) and **8c** ($\nu_{\text{CN}} = 1672 \text{ cm}^{-1}$). Convincing evidence for the structural assignments of **7c** and **8c** is found in the ¹H and ¹³C NMR spectra of these complexes. The most diagnostic features in the ¹H NMR spectra of **7c** and **8c** are the doublet resonances of the rhodium-bound methyl groups at 1.16 (²J_{Rh–H} = 2.0 Hz) and 1.18 (²J_{Rh–H} = 2.0 Hz), respectively. The ¹³C{¹H} resonances of these rhodium-bound methyl groups appear at –5.6 (¹J_{Rh–C} = 28.0 Hz) and –5.5 (¹J_{Rh–C} = 28.7 Hz) ppm in **7c** and **8c**, respectively. The appearance of four distinct diastereotopic resonances for the methyl protons of the isopropyl groups in the ¹H NMR spectra of **7c** and **8c** and the inequivalence of these carbon atoms in the ¹³C{¹H} NMR spectra are consistent with the reduced symmetry of these chloromethylrhodium complexes compared to the dichlororhodium complexes **3c** and **4c**.

Treatment of the chloromethylrhodium complex **7c** or **8c** with silver triflate led to quantitative formation of triflate complexes **9c** and **10c** as yellow, microcrystalline solids. For these triflate complexes, the methyl protons of the ligand isopropyl groups appear as four distinct diastereotopic resonances in the ¹H NMR spectra, suggesting that exchange of the triflate ligand is slow relative to the NMR time scale at room temperature. Yellow crystals of **9c** suitable for X-ray analysis were

(21) (a) van der Boom, M. E.; Higgit, C. L.; Milstein, D. *Organometallics* **1999**, *18*, 2413. (b) Vignalok, A.; Uzan, O.; Shimon, L. J. W.; Ben-David, Y.; Martin, J. M. L.; Milstein, D. *J. Am. Chem. Soc.* **1998**, *120*, 12539.

(22) van der Zeijden, A. A. H.; van Koten, G.; Ernsting, J. M.; Elsevier, C. J.; Krijnen, B.; Stam, C. H. *J. Chem. Soc., Dalton Trans.* **1989**, 317.

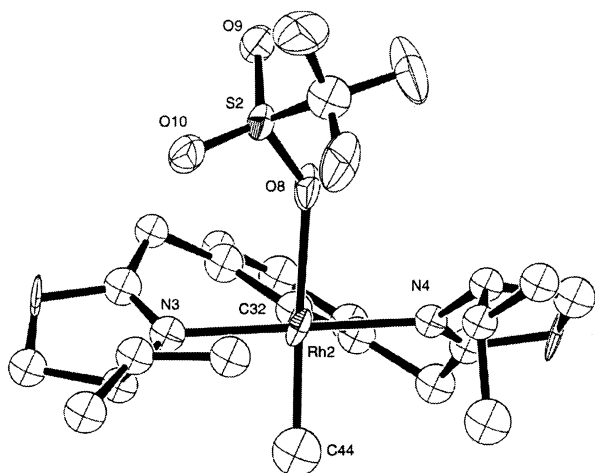


Figure 2. Molecular structure of one independent rhodium center from the crystal structure of **9c**. Hydrogen atoms are omitted for clarity. Thermal ellipsoids are shown at the 50% probability level.

Table 3. Selected Distances (Å) and Bond Angles (deg) for [Rh(OTf)Me{(S,S)-ip-benbox}] (9c**)**

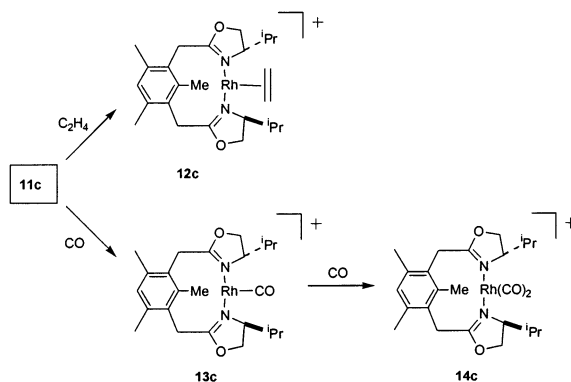
| | | | |
|-------------|---------|-------------------|----------|
| Rh(2)–N(3) | 2.08(1) | N(3)–Rh(2)–N(4) | 179.4(6) |
| Rh(2)–N(4) | 2.08(1) | O(8)–Rh(2)–C(44) | 172.3(8) |
| Rh(2)–O(8) | 2.28(1) | C(32)–Rh(2)–C(44) | 92.8(9) |
| Rh(2)–C(44) | 1.97(2) | O(8)–Rh(2)–C(32) | 94.6(7) |
| Rh(2)–C(32) | 1.90(2) | S(2)–O(8)–Rh(2) | 140.4(8) |

obtained by layering a concentrated CH_2Cl_2 solution of **9c** with pentane at room temperature. The compound crystallizes with four independent molecules of **9c** in the asymmetric unit, and the molecular structure of one of these is shown in Figure 2. Crystal data and structure refinement information is presented in Table 1, and representative bond lengths and angles for **9c** are given in Table 3. The molecular structure may be described as a square-based pyramid, with the methyl and triflate groups in a *trans* relationship. As was observed in **4c**, the Rh–N distances (2.08(1), 2.08(1) Å) are equivalent, and the N–Rh–N axis is effectively linear ($\text{N}(1)\text{--Rh}(1)\text{--N}(2) = 179.4(6)^\circ$).

When treated with NaBAR_f ($\text{BAR}_f = \text{tetrakis}\{(3,5\text{-trifluoromethyl})\text{phenyl}\}\text{borate}$), complex **10c** was converted to the tetraarylborate salt $[\text{RhMe}\{(S,S)\text{-ip-benboxMe}_2\}]\text{BAR}_f$ (**11c**). Complex **11c** was isolated in 97% yield as an air-sensitive, bright yellow microcrystalline solid. Decomposition was observed when methylene chloride solutions of **11c** were heated to temperatures above 72°C . The IR spectrum of **11c** contains a weak band at 2809 cm^{-1} , which is assigned to an agostic interaction of an isopropyl group with the cationic metal center. Much like the methylrhodium complexes **7c**–**10c**, the rhodium cation **11c** exhibits diastereotopic resonances for the isopropyl groups in the ^1H NMR spectrum, indicating that the compound is not C_2 -symmetric and, hence, that the methyl group resides in the apical coordination site.

Exposing methylene chloride solutions of **11c** to ethylene yielded the cationic (ethylene)rhodium(I) complex **12c**, apparently as a result of reductive elimination (Scheme 4). The formulation of complex **12c** shown in Scheme 4 is supported by the disappearance of the resonance of the rhodium-bound methyl group in the ^1H NMR spectrum and appearance of a resonance for a methyl group bound to the *ipso*-carbon of the ligand aryl

Scheme 4. Reductive Elimination Reactions



ring at 2.72 ppm. Two multiplet resonances at 3.50 and 3.27 ppm are assigned to the metal-bound ethylene ligand. The ^1H NMR spectrum of complex **12c** reveals four different doublet resonances for the ligand isopropyl groups, which is consistent with a decrease in symmetry of the rhodium cation caused by methyl migration. The reductive elimination reaction described for the formation of ethylene complex **12c** is similar to methyl migrations described by Milstein and van Koten for related PCP pincer complexes.^{21b,23}

In a related reaction, methylrhodium cation **11c** rapidly underwent methyl-arene reductive elimination when treated with carbon monoxide to give the monocarbonyl complex **13c** (Scheme 4). The spectroscopic features of **13c** are similar to those of the ethylene complex **12c**, with the proton resonance for the methyl group bound to the aryl *ipso*-carbon appearing at 2.86 ppm in **13c**. Due to rapid association of a second equivalent of CO, the monocarbonyl complex **13c** could not be isolated (*vide infra*).

The reaction between **11c** and carbon monoxide was allowed to proceed for 14 h at room temperature, and over this time period the monocarbonyl complex **13c** was completely converted to the dicarbonylrhodium(I) complex **14c**. The proton resonance for the *ipso*-carbon-bound methyl group appears at 2.40 ppm in the ^1H NMR spectrum of **14c**. On the basis of the IR stretching frequencies of the carbonyl ligands ($\nu_{\text{CO}} = 2094, 2029\text{ cm}^{-1}$), **14c** is formulated as a dicarbonyl and not an acyl complex (the product of insertion of CO into the Rh–CH₃ bond). To confirm this assignment, **14c** was synthesized with isotopically enriched ^{13}C . The IR spectrum of **14c**(^{13}C) displays $^{13}\text{C}\text{--O}$ stretching vibrations with the expected isotopic shifts ($\nu^{13}\text{CO} = 2052, 1993$). These data definitively confirm that **14c** is not a rhodium-acyl complex. Furthermore, in the $^{13}\text{C}\{^1\text{H}\}$ NMR spectrum of **14c**(^{13}C), two resonances at 180.3 and 179.9 ppm (dd, $^1J_{\text{Rh}\text{--C}} = 70\text{ Hz}$, $^2J_{\text{C}\text{--C}} = 6.3\text{ Hz}$) are assigned to the carbonyl carbon atoms.

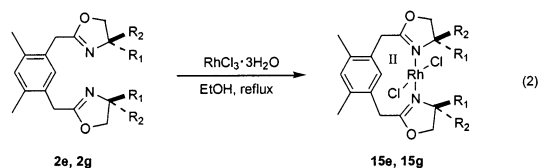
The formation of monocarbonyl complex **13c** is similar to processes described by Milstein for PCP pincer complexes.^{21b,23c} An important difference is the coordination of an additional equivalent of CO to form dicarbonyl complex **14c**. The monocarbonylrhodium PCP pincer compounds described by Milstein are sta-

(23) (a) Grove, D. M.; van Koten, G.; Louwen, J. N.; Noltes, J. G.; Spek, A. L.; Ubbels, H. J. C. *J. Am. Chem. Soc.* **1982**, *104*, 6609. (b) Terheijden, J.; van Koten, G.; Vrieze, K.; Vinke, I. C.; Spek, A. L. *J. Am. Chem. Soc.* **1985**, *107*, 2891. (c) Vigalok, A.; Milstein, D. *Organometallics* **2000**, *19*, 2341.

bilized by strong interactions between the rhodium and arene, leading to localization of the cationic charge on the aromatic system. These compounds do not associate additional carbon monoxide to form dicarbonyl complexes analogous to **14c**. Although a weak rhodium–arenium interaction may be present in **13c**, it does not prevent association of a second equivalent of CO. This difference may be related to the lesser steric demand of the isopropyl benboxMe₂ ligand of **13c** relative to Milstein's *tert*-butyl phosphine-substituted pincer ligand or to the increased conformational flexibility offered by the six-membered chelate ring of **13c** relative to the five-membered chelate ring of Milstein's complex.

Although the rhodium(III) pincer complexes **3** and **4** undergo a wide variety of interesting stoichiometric reactions, these compounds were found to be ineffective as catalysts for asymmetric transformations. Nishiyama's rhodium(III) pybox complexes catalyze hydrosilylation, and we had hoped to find analogous reactivity with the benbox rhodium(III) complexes.^{2b} Unfortunately, appreciable yields of hydrosilylation products were not observed in attempted catalytic reactions using the benbox rhodium complexes **4** with 1-hexene or acetophenone and phenylsilane or diphenylsilane. Similarly, attempts to catalyze allylation of benzaldehyde (a reaction achieved by the phebox complexes of rhodium(III)) with complex **4c** were unsuccessful.¹¹ We attribute this catalytic inactivity to the greater steric demands of the benbox ligands relative to the pybox and phebox ligands. Although the steric bulk of the ligand seems to limit the catalytic activity of the rhodium(III) complexes, it has allowed for the isolation of several unique and catalytically active rhodium(II) complexes (vide infra).

Synthesis and Characterization of Rhodium(II) Complexes. When the sterically demanding ligands **2e** and **2g** were heated with RhCl₃·3H₂O in ethanol, the monomeric rhodium(II) complexes **15e** (19%) and **15g** (49%) were formed in addition to the expected cyclometalated rhodium(III) complexes **4e** and **4g** (eq 2).



These complexes were cleanly separated by column chromatography. The yield of the *tert*-butyl-substituted rhodium(II) complex **15e** was improved by running the reaction at high dilution, giving an optimized yield of 57%.

X-ray quality crystals were obtained by cooling a concentrated toluene/pentane solution of **15g**. The molecular structure of **15g** is shown in Figure 3. Crystal data and structure refinement information is presented in Table 1, and selected interatomic distances and bond angles are given in Table 4. The complex crystallizes as discrete molecules with no noticeable interatomic interactions. The geometry at the rhodium center is approximately square-planar (maximum deviation of 0.137(2) Å by Cl(2) for the Rh(1)Cl(1)Cl(2)N(1)N(2) least squares plane). The Rh–Cl distances (2.356(2)/2.365(1) Å) are equivalent within 3σ, as are the Rh–N

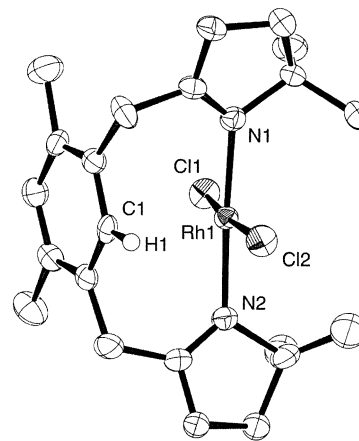


Figure 3. Molecular structure of **15g**. Hydrogen atoms are omitted for clarity. Thermal ellipsoids are shown at the 50% probability level.

Table 4. Selected Distances (Å) and Bond Angles (deg) for [RhCl₂{dm-benbox(Me₂)}] (**15g**)

| | | | |
|--------------|----------|-------------------|-----------|
| Rh(1)–Cl(1) | 2.336(2) | Cl(1)–Rh(1)–Cl(2) | 173.1 (5) |
| Rh(1)–Cl(2) | 2.364(1) | N(1)–Rh(1)–N(2) | 176.1(1) |
| Rh(1)–N(1) | 2.074(4) | Cl(1)–Rh(1)–N(1) | 92.6 (1) |
| Rh(1)–N(2) | 2.072(4) | Cl(1)–Rh(1)–N(2) | 90.5 (1) |
| Rh(1)···C(1) | 2.575(5) | | |

distances (2.074(4)/2.072(4) Å). The phenyl group of the ligand defined by the carbon atoms C(1)–C(6) is roughly parallel (17°) to the coordination plane of the rhodium. The distance between the rhodium center and the nearest aryl carbon (C(1)) is 2.575(5) Å, indicating that a weak agostic interaction may exist between these two atoms. This rhodium–carbon distance is significantly longer than that in a related “PCP pincer” rhodium(I) complex containing an η² agostic Rh···C–H bond (2.273(5) Å).^{21b} The carbon–carbon bond distances in the phenyl ring range from 1.362(8) to 1.4223(8) Å, showing a slight distortion from aromaticity.

The paramagnetism of complexes **15e,g** was established by several spectroscopic and magnetic techniques. The ¹H NMR spectra of the complexes contain only broad resonances, which range between 37 and –33 ppm for each compound. In the infrared spectra, the C–N stretching vibrations appear at lower frequencies (**15e**: 1647, 1637 cm^{–1}; **15g**: 1654, 1641 cm^{–1}) than those in the corresponding rhodium(III) complexes **4e** (1670 cm^{–1}) and **4g** (1680 cm^{–1}) and those in the uncoordinated bis(oxazolines) **2e** (1665 cm^{–1}) and **2g** (1659 cm^{–1}). The observed shift in the infrared spectra is consistent with the increased electron-richness of the rhodium(II) centers over rhodium(III) centers.

The rhodium(II) complexes **15e,g** exhibit nearly identical cyclic voltammograms. Cyclic voltammetry was performed with a platinum electrode over the scan rate range of 10–1000 mV·s^{–1} at room temperature in dichloromethane solution with 0.1 M [NBu₄]PF₆. One irreversible oxidation wave (Rh(II)/Rh(III)) was observed at +0.68 V (100 mV/s) for **15e** and at +0.80 V (100 mV/s) for **15g**. In addition, irreversible reduction processes (Rh(II)/Rh(I)) were observed at –1.43 V for **15e** and at –1.44 V for **15g**.

X-band EPR spectra for **15e,g** were obtained in glassy frozen 2-methyltetrahydrofuran, yielding *g*-values of *g*₁ = 2.864, *g*₂ = 2.320, and *g*₃ = 1.903 for **15e** (spectrum obtained at 57 K) (Figure 4). Doublet splitting from the

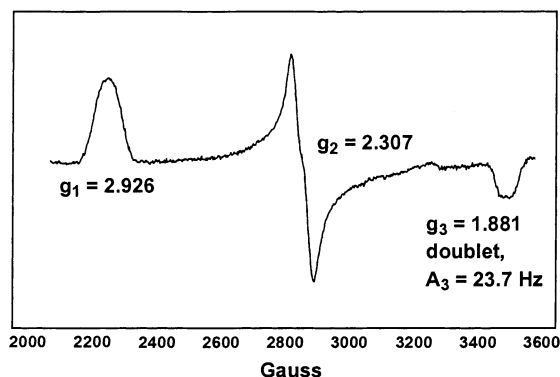


Figure 4. X-band EPR spectrum of **15g** obtained at 57 K in glassy frozen THF.

hyperfine interaction with ^{103}Rh ($I = 1/2$) was observed for g_2 ($A_2 = 14.5$ G) and g_3 ($A_3 = 28.3$ G). Complex **15g** also shows three g values: $g_1 = 2.926$, $g_2 = 2.307$, and $g_3 = 1.881$ (spectrum obtained at 1.2 K). For **15g**, hyperfine coupling to ^{103}Rh of only g_3 is observed (doublet; $A_3 = 23.7$ Hz; Figure 4). The EPR spectra acquired for **15e,g** are rhombic, consistent with the asymmetric coordination environments around the metal centers in these complexes.

The magnetic properties of **15g** were investigated using SQUID magnetometry. Complex **15g** exhibits clean Curie–Weiss behavior between 5 and 289 K, with an average magnetic moment of $2.00(2) \mu_{\text{B}}$. The solution paramagnetism of the rhodium(II) complexes, determined by the Evans method, yielded μ_{eff} values of $1.87 \mu_{\text{B}}$ (**15e**) and $1.98 \mu_{\text{B}}$ (**15g**).²⁴ The solid and solution phase magnetic measurements are both consistent with an $S = 1/2$ ground state, as expected for a monomeric low-spin d^7 metal complex. The electronic spectra of complexes **15e,g** display three major bands at $\lambda_{\text{max}} = 410$, 309, and 229 nm for **15e** and at $\lambda_{\text{max}} = 405$, 303, and 231 nm for **15g**. Bands similar to those observed for **15e,g** have been noted for other four-coordinate monomeric rhodium(II) complexes. In these complexes, bands near 300 nm have been assigned to ligand-based $\pi-\pi^*$ transitions, and those near 400 nm have been assigned to a ligand-to-metal charge transfer.²⁵ No bands indicative of $d-d$ transitions were observed in the visible region of the spectrum.^{25,26}

The chemistry of rhodium is generally associated with the oxidation states +1 and +3. Although many rhodium(II) dimers have been characterized,²⁷ far fewer monomeric rhodium(II) complexes have been isolated.^{25,26,28} In contrast to the vast majority of compounds containing mononuclear rhodium(II) centers, complexes **15e,g** are air-stable and melt cleanly at temperatures above 180 °C. The stability of complexes **15e** and **15g** is presumably due to their sterically congested ligand environments.

The formation of rhodium(II) products from ethanolic solutions of $\text{RhCl}_3(\text{H}_2\text{O})_3$ and bulky ligands has been observed previously. These reactions are assumed to occur via oxidation of the ethanol solvent or excess ligand, although the mechanisms have not been studied.^{25,28c}

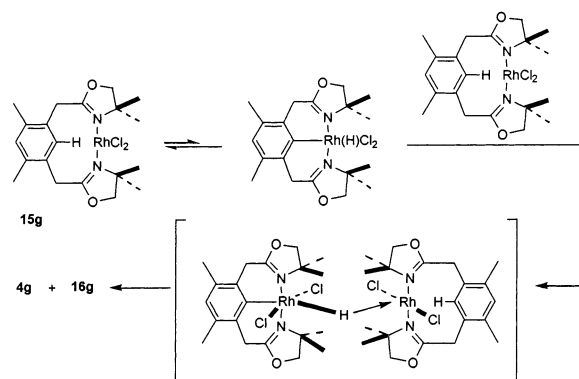
(24) (a) Evans, D. F. *J. Chem. Soc.* **1959**, 2003. (b) Evans, D. A.; Miller, S. J.; Lectka, T. *J. Am. Chem. Soc.* **1993**, *115*, 6460.

(25) Pandey, K. K. *Coord. Chem. Rev.* **1992**, *121*, 1.

(26) Dunbar, K. R.; Haefner, S. C. *Organometallics* **1992**, *11*, 1431.

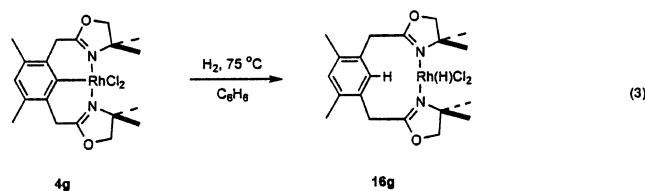
(27) Doyle, M. P.; Forbes, D. C. *Chem. Rev.* **1998**, *98*, 911.

Scheme 5. Proposed Mechanism for Disproportionation



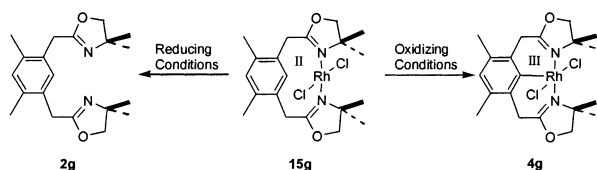
The reactions that form **15e,g** are heterogeneous (an orange precipitate forms as the reaction progresses), which prohibits the use of kinetic tools to study the mechanisms in detail. Complex **15e** is isolated in higher yield under dilute synthesis conditions, suggesting that a dinuclear decomposition pathway is competitive with formation of **15e,g** (vide infra).

Stoichiometric Reactivity of Rhodium(II) Complexes. When concentrated solutions of **15g** are heated to 75 °C in benzene solution, disproportionation to cyclo-metallated rhodium(III) dichloride **4g** and hydridorhodium(III) dichloride **16g** is observed (Scheme 5). The identity of the hydridorhodium(III) complex **16g** was confirmed by independent synthesis (eq 3). When a



benzene solution of **4g** was treated with 35 atm H_2 , complete conversion to **16g** was observed after 14 h at 75 °C. The hydridorhodium(III) compound was cleanly isolated in 75% yield as an analytically pure yellow powder. The chemistry and full characterization of **16g** and a series of related hydridorhodium complexes will be fully described in a future publication.

(28) (a) DeWitt, D. G. *Coord. Chem. Rev.* **1996**, *147*, 209. (b) Billig, E.; Shupack, S. I.; Waters, J. H.; Williams, R.; Gray, H. B. *J. Am. Chem. Soc.* **1964**, *86*, 926. (c) Bennett, M. A.; Longstaff, P. A. *J. Am. Chem. Soc.* **1969**, *91*, 6266. (d) Masters, C.; Shaw, B. L. *J. Chem. Soc. A* **1971**, 3679. (e) Dunbar, K. R.; Haefner, S. C.; Pence, L. E. *J. Am. Chem. Soc.* **1989**, *111*, 5504. (f) Haefner, S. C.; Dunbar, K. R.; Bender, C. J. *J. Am. Chem. Soc.* **1991**, *113*, 9540. (g) Wayland, B. B.; Ba, S.; Sherry, A. E. *J. Am. Chem. Soc.* **1991**, *113*, 5305. (h) Zhang, X. X.; Wayland, B. B. *J. Am. Chem. Soc.* **1994**, *116*, 7897. (i) Bunn, A. G.; Wayland, B. B. *J. Am. Chem. Soc.* **1992**, *114*, 6917. (j) Bunn, A. G.; Wei, M. L.; Wayland, B. B. *Organometallics* **1994**, *13*, 3390. (k) Connelly, N. G.; Emslie, D. J. H.; Metz, B.; Orpen, A. G.; Quayle, M. J. *Chem. Commun.* **1996**, 2289. (l) Zhang, X. X.; Parks, G. F.; Wayland, B. B. *J. Am. Chem. Soc.* **1997**, *119*, 7938. (m) Parimal, P.; Tyagi, B.; Bilakhiya, A. K.; Bhadbhade, M. M.; Suresh, E. *J. Chem. Soc., Dalton Trans.* **1999**, 2009. (n) Collman, J. P.; Boulatov, R. *J. Am. Chem. Soc.* **2000**, *122*, 11812. (o) Connelly, N. G.; Emslie, D. J. H.; Geiger, W. E.; Hayward, O. D.; Linehan, E. B.; Orpen, A. G.; Quayle, M. J.; Rieger, P. H. *J. Chem. Soc., Dalton Trans.* **2001**, 670. (p) Willems, S. T. H.; Russcher, J. C.; Budzelaar, P. H. M.; de Bruin, B.; de Gelder, R.; Smits, J. M. M.; Gal, A. W. *Chem. Commun.* **2002**, 148. (q) Dixon, F. M.; Farrell, J. R.; Doan, P. E.; Williamson, A.; Weinberger, D. A.; Mirkin, C. A.; Stern, C.; Incarvito, C. D.; Liable-Sands, L. M.; Zakharov, L. N.; Rheingold, A. L. *Organometallics* **2002**, *21*, 3091.

Scheme 6. Reactions of Rhodium(II) Complex **15g**

The decomposition of **15g** to **4g** and **16g** presumably occurs via a bimolecular hydrogen transfer reaction. A suggested mechanism for the decomposition reaction is illustrated in Scheme 5. A rapid, reversible C–H activation of the proximal ligand aryl C–H bond is proposed as the first step. C–H activation reactions have been observed previously with rhodium(II) porphyrin complexes, although these reactions are typically thought to involve concerted action of two rhodium(II) centers.^{28g} The proposed decomposition mechanism invokes a dinuclear step to accomplish the one-electron oxidation process. Unfortunately, this reaction was not amenable to kinetic study due to the slow precipitation of rhodium metal that is observed during its course.

Reactions of complex **15g** with several reducing agents (trimethylphosphine, sodium, magnesium, *tert*-butylisonitrile, and pyridine or Bu₃SnH) led to clean formation of free ligand **2g** and unidentifiable rhodium products (Scheme 6). The rhodium(III) complex **4g** was obtained in 56% yield by exposing a benzene-*d*₆ solution of **15g** to 800 mbar of O₂ and heating to 45 °C for 2 days, or in 92% yield by heating a benzene-*d*₆ solution of **15g** with CCl₄ at 75 °C for 6 days, or in 80% yield by reaction of **15g** with CuCl₂ in methylene chloride at room temperature for 2 days (Scheme 6). These reactions demonstrate that it is possible to oxidize the hindered rhodium(II) complex by chemical means, despite the compound's stability to air. No reaction was observed when complex **15g** was treated with benzyl chloride, triethylamine, methane, methyl iodide, acetonitrile, *tert*-butyl nitrile, or lead dichloride.

A few monomeric 15e⁻ rhodium(II) complexes have been described previously (either as isolable compounds or as transiently generated species).^{26,28h,n,29} Several of these compounds react readily with donor ligands (CO, nitriles, phosphines) to form 17e⁻ complexes or undergo redox processes.^{28h,n,29a} Given this precedent, the lack of similar trapping reactions (*vide supra*) with **15g** is somewhat surprising. This result is similar to the observation that the rhodium(III) complexes (**4a–g**) in this ligand series are isolated as water-free 16e⁻ complexes. The steric bulk of the ligand presumably inhibits coordination of additional ligands in the open coordination sites of both the rhodium(II) and rhodium(III) complexes.

Conclusion

We have prepared a series of new NCN bis(oxazoline) pincer ("benbox") ligands and used these ligands to prepare unique, coordinatively unsaturated rhodium(III) compounds and mononuclear rhodium(II) complexes. The ligands are readily synthesized from commercially available amino alcohols, providing easy

access to chiral metal complexes. Although the rhodium(III) complexes were found to be inactive for catalysis, a variety of rare and interesting new compounds were isolated and fully characterized. The 16-electron rhodium(III) dichloride complexes are stabilized by agostic interactions with the ligand alkyl groups and can be trapped by several nucleophilic ligands to give coordinatively saturated complexes. Methylrhodium(III) cationic complexes were synthesized and were shown to undergo 1,2-methyl migration reactions similar to those described by Milstein and van Koten. Importantly, the most sterically demanding benbox ligands allowed for isolation of mononuclear rhodium(II) complexes, which were extensively characterized in the solid and solution phases. Further studies of the catalytic reactivity of the rhodium(II) compounds are currently underway in our laboratories.

Experimental Section

General Procedures. Unless otherwise noted, reactions and manipulations were performed at 23 °C in an inert atmosphere (N₂) glovebox, or using standard Schlenk and high-vacuum line techniques. Glassware was dried overnight at 150 °C before use. All NMR spectra were obtained using Bruker AMX-300, AM-400, or DRX-500 MHz spectrometers. Except where noted, all NMR spectra were acquired at room temperature. Infrared (IR) spectra were recorded using samples prepared as KBr pellets, and spectral data are reported in wavenumbers. Reactions with gases and low-boiling liquids involved condensation of a calculated pressure of gas from a bulb of known volume into the reaction vessel at –196 °C. Known-volume bulb vacuum transfers were accomplished with a digital MKS Baratron gauge attached to a high-vacuum line.

Mass spectrometric (MS) analyses were obtained at the University of California, Berkeley Mass Spectrometry Facility, on VT ProSpec, ZAB2-EQ, and 70-FE mass spectrometers. Unless otherwise noted, all FABMS data were acquired from samples in a methylene chloride/3-nitrobenzyl alcohol matrix. Elemental analyses were performed at the University of California, Berkeley Microanalytical Facility, on a Perkin-Elmer 2400 Series II CHNO/S analyzer. Optical rotation measurements were performed on a Perkin-Elmer polarimeter (sodium D line). X-band EPR spectra of samples in glassy 2-methyltetrahydrofuran were recorded in deoxygenated EPR tubes at both 57 and 1.2 K on a Bruker EMX-300 EPR.

All electrochemical experiments were performed with a Bioanalytical Systems (BAS) CV-50W voltammetric analyzer at room temperature using a Pt working electrode (area = 0.03 cm²), a Pt-wire auxiliary electrode, and a BAS nonaqueous Ag/AgNO₃ reference electrode containing 0.01 M AgNO₃ in a 0.1 M tetra-*n*-butylammonium hexafluorophosphate (TBAH) methylene chloride solution. A normal three-electrode configuration was used, and the cell contained a 0.3 M solution of supporting electrolyte (TBAH) in THF. All potentials are reported versus Ag/AgNO₃ and were not corrected for liquid junction potential. The standard current convention is used (anodic currents are negative). Potentials measured versus the ferrocene/ferrocenium couple, Fc^{0/+}, were obtained by external calibration, due to the reactivity of the compounds with ferrocene. Controlled potential coulometry experiments were carried out on stirred solutions using a vitreous carbon electrode, a Pt auxiliary electrode, and a nonaqueous Ag/AgNO₃ reference electrode. The auxiliary electrode was separated from the working compartment by a fritted glass salt bridge.

Materials. Unless otherwise noted, reagents were purchased from commercial suppliers and used without further purification. Pentane, hexanes, methylene chloride, and benzene (Fisher) were passed through a column of activated

(29) (a) Poszmiak, G.; Carroll, P. J.; Wayland, B. B. *Organometallics* **1993**, *12*, 3410. (b) Wayland, B. B.; Sherry, A. E.; Bunn, A. G. *J. Am. Chem. Soc.* **1993**, *115*, 7675.

alumina (type A2, size 12 × 32, Purifry Co.) under nitrogen pressure and sparged with N₂ prior to use. Diethyl ether and tetrahydrofuran (Fisher) were distilled from purple sodium/benzophenone ketyl under N₂ prior to use. Deuterated solvents (Cambridge Isotope Laboratories) were either purified by vacuum transfer from the appropriate drying agent (Na/Ph₂CO or CaH₂) prior to use (C₆D₆, CD₂Cl₂) or used as received (CDCl₃). Chlorobenzene and dimethyl sulfoxide were used as received under nitrogen. Trimethylphosphine (Aldrich) was vacuum-transferred from sodium metal prior to use. Tetra-*n*-butylammonium hexafluorophosphate (Aldrich) was dried under vacuum for 24 h and stored in a glovebox. Spectral and analytical data for compounds **1b–g**, **2b–g**, **3d–g**, and **4e–g** are provided in the Supporting Information.

1,3-Bis(chloromethyl)-4,6-dimethylbenzene.¹⁶ A 1 L three-necked flask was loaded with *m*-xylene (20 mL, 164 mmol), paraformaldehyde (11.6 g, 363 mmol), 160 mL of concentrated hydrochloric acid, and 40 mL of glacial acetic acid. The mixture was heated at 69–70 °C for 2 days, over which time the solution turned colorless and a white precipitate formed. The solution was filtered and extracted with methylene chloride (5 × 50 mL). The organic phases were combined and rinsed with aqueous 10% NaHCO₃ solution (3 × 50 mL) and water (3 × 50 mL). The organic phase was dried with sodium sulfate, filtered, and evaporated to dryness in vacuo to give a white solid. The product was purified by crystallization from hexane. Yield: 21.1 g, 63%. Mp: 95 °C. ¹H NMR (300 MHz, C₆D₆): δ 6.76 (s, 1H, CH), 6.59 (s, 1H, CH), 4.07 (s, 4H, CH₂), 2.03 (s, 6H, CH₃). ¹³C{¹H} NMR (101 MHz, C₆D₆): δ 138.2, 134.1, 133.6, 131.9, 44.7, 18.5.

(4,6-Dimethyl-*m*-phenylene)diacetonitrile.¹⁷ In a 500 mL round-bottom flask, 10.8 g (220 mmol) of sodium cyanide was dried under vacuum at 100 °C for 30 min. The flask was cooled to 10–15 °C, and dry dimethyl sulfoxide (200 mL) was added carefully over 5 min. After this time, 20.3 g (100 mmol) of 1,3-bis(chloromethyl)-4,6-dimethylbenzene was added over 10 min, producing a light yellow suspension. The mixture was heated with stirring at 40–50 °C for 2 h. After cooling to 25 °C, this suspension was poured onto 1 L of water, then extracted with benzene (6 × 80 mL). The combined organic extracts were dried over sodium sulfate. After filtration, the solvent was removed by rotary evaporation to give a yellow oil. Methanol (50 mL) was added to the oil, and the mixture was cooled to 0 °C. Colorless crystals precipitated and were collected by filtration. Yield: 13.8 g, 75%. Mp: 88–90 °C. ¹H NMR (300 MHz, C₆D₆): δ 7.27 (s, 1H, CH), 7.07 (s, 1H, CH), 3.64 (s, 4H, CH₂), 2.32 (s, 6H, CH₃). ¹³C{¹H} NMR (101 MHz, C₆D₆): δ 136.3, 133.2, 129.3, 127.8, 21.1, 18.7.

General Procedure for the Preparation of Ligands 1 and 2. A 250 mL three-necked flask was charged with Cd(OAc)₂·2H₂O (266 mg, 1.0 mmol), 20 mmol of the appropriate dinitrile, 75 mmol of the appropriate amino alcohol, and 80 mL of chlorobenzene. The mixture was heated at reflux for 2–6 days under nitrogen. The solvent was removed under reduced pressure, giving an oily residue. The residue was purified by flash chromatography on silica gel (gradient 50%–80% ethyl acetate/hexane) to afford the desired bis(2-oxazoline) as either an off-white solid or a light yellow oily solid.

1,3-Bis[4'-(*S*-methyloxazolin-2'-yl)methyl]benzene, (*S,S*)-*me*-benbox (1a**):** off-white solid, yield 3.54 g, 65%. Mp: 56–58 °C. *R*_f = 0.03 (ethyl acetate). [α]_D = –39.6°. Anal. Calcd for C₁₆H₂₀N₂O₂: C, 70.58; H, 7.40; N, 10.29. Found: C, 70.88; H, 7.39; N, 10.17. IR (KBr, cm^{–1}): 1661 (ν_{CN}). ¹H NMR (300 MHz, CDCl₃): δ 7.21–7.09 (m, 4H, CH), 4.18 (dd, 2H, ox-CH₂), 4.06 (m, 2H, ox-CH), 3.62 (dd, 2H, ox-CH₂), 3.46 (s, 4H, CH₂), 1.13 (d, 6H, CH₃). ¹³C{¹H} NMR (126 MHz, CDCl₃): δ 164.9, 134.9, 128.9, 128.1, 126.9, 73.5, 60.8, 34.0, 20.8.

1,3-Bis[4'-(*S*-methyloxazolin-2'-yl)methyl]-4,6-dimethylbenzene, (*S,S*)-*me*-benbox(Me₂) (2a**):** off-white solid, yield 3.27 g, 63%. Mp: 58–59 °C. *R*_f = 0.12 (ethyl acetate). [α]_D = –50.7°. Anal. Calcd for C₁₈H₂₄N₂O₂: C, 71.97; H, 8.05;

N, 9.32. Found: C, 71.81; H, 8.05; N, 9.32. IR (KBr, cm^{–1}): 1663 (ν_{CN}). ¹H NMR (300 MHz, CDCl₃): δ 7.08 (s, 1H, CH), 6.97 (s, 1H, CH), 4.30 (dd, 2H, ox-CH₂), 4.14 (m, 2H, ox-CH), 3.76 (dd, 2H, ox-CH₂), 3.56 (s, 4H, CH₂), 2.27 (s, 6H, CH₃), 1.23 (d, 6H, ox-CH₃). ¹³C{¹H} NMR (126 MHz, CDCl₃): δ 165.5, 135.7, 132.5, 131.4, 131.2, 74.0, 61.4, 32.3, 21.4, 19.1.

General Procedure for Preparation of Rhodium Complexes 3 and 4. To a solution of the bis(oxazoline) **1** or **2** (1.3 mmol) in 10 mL of degassed ethanol at 70 °C was added RhCl₃·3H₂O (263 mg, 1.0 mmol). The resulting orange-red suspension was heated at reflux for 5–30 min. After evaporation to dryness at room temperature the product was isolated by column chromatography on silica (CH₂Cl₂) as an air-stable orange-red microcrystalline solid.

[RhCl₂{(*S,S*)-*me*-benbox}] (3a**):** yield 84 mg, 19% (30 min reflux). Mp: >260 °C. *R*_f = <0.01 (methylene chloride). Anal. Calcd for C₁₆H₁₉Cl₂N₂O₂Rh: C, 43.17; H, 4.30; N, 6.29. Found: C, 42.91; H, 4.31; N, 5.98. IR (KBr, cm^{–1}): 1668 (ν_{CN}). ¹H NMR (300 MHz, C₆D₆): δ 6.80 (t, 1H, CH), 6.56 (d, 2H, CH), 4.78 (d, 2H, CH₂, ²J_{H–H} = 17.7 Hz), 4.60 (m, 2H, ox-CH), 3.69 (dd, 2H, ox-CH₂), 3.44 (d, 2H, CH₂, ²J_{H–H} = 17.7 Hz), 3.35 (t, 2H, ox-CH₂), 1.38 (d, 6H, ox-CH₃). ¹³C{¹H} NMR (126 MHz, CDCl₃): δ 170.5, 139.0, 131.4 (d, ¹J_{Rh–C} = 34.5 Hz), 127.6, 124.8, 76.2, 59.9, 36.3, 20.8.

[RhCl₂{(*S,S*)-*et*-benbox}] (3b**):** yield 180 mg, 38% (30 min reflux). Mp: >260 °C. *R*_f = 0.27 (methylene chloride). Anal. Calcd for C₁₈H₂₃Cl₂N₂O₂Rh: C, 45.69; H, 4.90; N, 5.92. Found: C, 45.53; H, 4.71; N, 5.83. IR (KBr, cm^{–1}): 1677 (ν_{CN}). ¹H NMR (300 MHz, C₆D₆): δ 6.76 (t, 1H, CH), 6.53 (d, 2H, CH), 4.98 (d, 2H, CH₂, ²J_{H–H} = 17.6 Hz), 4.47 (m, 2H, ox-CH), 3.59 (dd, 2H, ox-CH₂), 3.47 (t, 2H, ox-CH₂), 3.28 (d, 2H, CH₂, ²J_{H–H} = 17.6 Hz), 1.73 (sept, 2H, Et-CH₂), 1.56 (sept, 2H, Et-CH₂), 1.08 (d, 6H, CH₃). ¹³C{¹H} NMR (126 MHz, CDCl₃): δ 170.5, 140.1 (d, ²J_{Rh–C} = 2.1 Hz), 134.6 (d, ¹J_{Rh–C} = 34.5 Hz), 127.7, 124.7, 73.8, 65.3, 36.9, 27.8, 11.4.

[RhCl₂{(*S,S*)-*ip*-benbox}] (3c**):** yield 295 mg, 59% (30 min reflux). Mp: >260 °C. *R*_f = 0.42 (methylene chloride). Anal. Calcd for C₂₀H₂₇Cl₂N₂O₂Rh: C, 47.92; H, 5.43; N, 5.59. Found: C, 47.91; H, 5.51; N, 5.70. IR (KBr, cm^{–1}): 1674 (ν_{CN}). ¹H NMR (300 MHz, C₆D₆): δ 6.76 (t, 1H, CH), 6.54 (d, 2H, CH), 5.05 (d, 2H, CH₂, ²J_{H–H} = 16.8 Hz), 4.52 (m, 2H, ox-CH), 3.69 (t, 2H, ox-CH₂), 3.57 (t, 2H, ox-CH₂), 3.29 (d, 2H, CH₂, ²J_{H–H} = 16.8 Hz), 2.10 (sept, 2H, *i*-Pr-CH), 1.03 (d, 6H, CH₃), 0.97 (d, 6H, CH₃). ¹³C{¹H} NMR (126 MHz, CDCl₃): δ 170.6, 139.5 (d, ²J_{Rh–C} = 1.6 Hz), 133.3 (d, ¹J_{Rh–C} = 36.9 Hz), 127.9, 125.1, 71.7, 69.4, 36.4, 31.3, 20.1, 17.4.

[RhCl₂{(*S,S*)-*me*-benbox(Me₂)}] (4a**):** yield 227 mg, 48% (30 min reflux). Mp: >260 °C. *R*_f = 0.05 (methylene chloride). Anal. Calcd for C₁₈H₂₃Cl₂N₂O₂Rh: C, 45.69; H, 4.90; N, 5.92. Found: C, 45.67; H, 5.10; N, 5.74. IR (KBr, cm^{–1}): 1676 (ν_{CN}). ¹H NMR (300 MHz, C₆D₆): δ 6.52 (s, 1H, CH), 4.63 (d, 2H, CH₂, ²J_{H–H} = 17.6 Hz), 4.53 (m, 2H, ox-CH), 3.64 (d, 2H, CH₂, ²J_{H–H} = 17.6 Hz), 3.61 (t, 2H, ox-CH₂), 3.33 (t, 2H, ox-CH₂), 1.88 (s, 6H, CH₃), 1.39 (d, 6H, ox-CH₃). ¹³C{¹H} NMR (126 MHz, CDCl₃): δ 170.5, 135.0 (d, ²J_{Rh–C} = 2.1 Hz), 133.7, 130.5, 130.3 (d, ¹J_{Rh–C} = 36.8 Hz), 76.1, 59.7, 31.4, 21.3, 20.8. FAB-MS (*m/z*): 437.1 [M – HCl]⁺, 402.1 [M – HCl – Cl]⁺.

[RhCl₂{(*S,S*)-*et*-benbox(Me₂)}] (4b**):** yield 250 mg, 50% (30 min reflux). Mp: >260 °C. *R*_f = 0.25 (methylene chloride). Anal. Calcd for C₂₀H₂₇Cl₂N₂O₂Rh: C, 47.92; H, 5.43; N, 5.59. Found: C, 47.62; H, 5.65; N, 5.53. IR (KBr, cm^{–1}): 1676 (ν_{CN}). ¹H NMR (300 MHz, C₆D₆): δ 6.55 (s, 1H, CH), 4.79 (d, 2H, CH₂, ²J_{H–H} = 17.6 Hz), 4.53 (m, 2H, ox-CH), 3.65 (d, 2H, CH₂, ²J_{H–H} = 17.6 Hz), 3.61 (t, 2H, ox-CH₂), 3.51 (t, 2H, ox-CH₂), 1.92 (s, 6H, CH₃), 1.76 (sept, 2H, Et-CH₂), 1.61 (sept, 2H, Et-CH₂), 1.11 (t, 6H, Et-CH₃). ¹³C{¹H} NMR (126 MHz, C₆D₆): δ 171.5, 136.4 (d, ²J_{Rh–C} = 2.1 Hz), 135.6 (d, ¹J_{Rh–C} = 36.8 Hz), 134.2, 130.3, 74.6, 66.1, 32.9, 28.7, 22.0, 12.1. FABMS (*m/z*): 500.1 [M]⁺, 465.1 [M – Cl]⁺, 429.2 [M – Cl – HCl]⁺.

[RhCl₂{(*S,S*)-*ip*-benbox(Me₂)}] (4c**):** yield 319 mg, 52% (30 min reflux). Mp: >260 °C. *R*_f = 0.49 (methylene chloride).

Anal. Calcd for $C_{22}H_{31}Cl_2N_2O_2Rh \cdot CH_2Cl_2$: C, 44.97; H, 5.42; N, 4.56. Found: C, 45.06; H, 5.68; N, 4.48. IR (KBr, cm^{-1}): 1680 (ν_{CN}). 1H NMR (300 MHz, C_6D_6): δ 6.54 (s, 1H, *CH*), 4.92 (d, 2H, CH_2 , $^2J_{H-H} = 17.5$ Hz), 4.60 (m, 2H, *ox-CH*), 3.74 (t, 2H, *ox-CH_2*), 3.69 (d, 2H, CH_2 , $^2J_{H-H} = 17.5$ Hz), 3.61 (t, 2H, *ox-CH_2*), 2.17 (sept, 2H, *i-Pr-CH*), 1.94 (s, 6H, CH_3), 1.08 (d, 6H, *i-Pr-CH_3*), 1.01 (d, 6H, *i-Pr-CH_3*). $^{13}C\{^1H\}$ NMR (126 MHz, C_6D_6): δ 171.0, 136.4 (d, $^2J_{Rh-C} = 2.0$ Hz), 135.5 (d, $^1J_{Rh-C} = 36.9$ Hz), 133.4, 130.3, 71.3, 69.4, 32.0, 31.6, 21.2, 19.8, 17.8. FABMS (m/z): 493.1 $[M - Cl]^+$, 457.1 $[M - 2HCl]^+$.

[RhCl₂{(S,S)-ib-benbox(Me₂)}] (4d): yield 228 mg, 41% (30 min reflux). Mp: >260 °C. $R_f = 0.45$ (methylene chloride). Anal. Calcd for $C_{24}H_{35}Cl_2N_2O_2Rh$: C, 51.72; H, 6.33; N, 5.03. Found: C, 51.46; H, 6.49; N, 4.92. IR (KBr, cm^{-1}): 2764, 2756 (ν_{CH}), 1683 (ν_{CN}). 1H NMR (300 MHz, C_6D_6): δ 6.54 (s, 1H, *CH*), 4.82 (d, 2H, CH_2 , $^2J_{H-H} = 17.0$ Hz), 4.58 (m, 2H, *ox-CH*), 3.70 (d, 2H, CH_2 , $^2J_{H-H} = 17.0$ Hz), 3.67 (t, 2H, *ox-CH_2*), 3.50 (t, 2H, *ox-CH_2*), 2.02 (sept, 2H, *i-Bu-CH*), 1.96 (s, 6H, CH_3), 1.54 (sept, 2H, *i-Bu-CH_2*), 1.20 (dt, 2H, *i-Bu-CH_2*), 1.08 (d, 6H, *i-Bu-CH_3*), 1.04 (d, 6H, *i-Bu-CH_3*). $^{13}C\{^1H\}$ NMR (126 MHz, C_6D_6): δ 170.4, 136.1 (d, $^2J_{Rh-C} = 2.2$ Hz), 134.8 (d, $^1J_{Rh-C} = 37.5$ Hz), 133.3, 130.2, 74.6, 62.8, 44.8, 32.1, 27.9, 22.7 (2 \times), 21.2. FABMS (m/z): 520.2 $[M - HCl]^+$, 485.2 $[M - Cl - HCl]^+$.

[RhCl₂{(S,S)-ib-benbox(Me₂)}(CO)] (5d). An orange solution of $[RhCl_2\{(S,S)\text{-ib-benbox(Me}_2)\}]$ (4d) (55.7 mg, 0.10 mmol) in benzene (10 mL) was exposed to 1 atm of CO at ambient temperature. This solution was heated at 75 °C, producing a light yellow suspension within 3 days. The volatile materials were removed under reduced pressure, and the resulting pale orange solid was washed with pentane (3 \times 10 mL). Anal. Calcd for $C_{25}H_{35}Cl_2N_2O_2Rh$: C, 51.30; H, 6.03; N, 4.79. Found: C, 51.68; H, 6.35; N, 4.43. IR (KBr, cm^{-1}): 2070 (ν_{CO}), 1666 (ν_{CN}). 1H NMR (300 MHz, C_6D_6): δ 6.61 (s, 1H, *CH*), 5.21 (m, 2H, *ox-CH*), 4.99 (d, 1H, CH_2 , $^2J_{H-H} = 14.4$ Hz), 3.85–3.54 (m, 6H, CH_2 , *ox-CH_2*), 3.37 (d, 1H, CH_2 , $^2J_{H-H} = 14.7$ Hz), 2.38 (dt, 1H, *i-Bu-CH*), 1.93 (s, 3H, CH_3), 1.90 (s, 3H, CH_3), 1.33 (dt, 1H, *i-Bu-CH*), 1.25–1.11 (m, 4H, *i-Bu-CH_2*), 1.07 (d, 3H, *i-Bu-CH_3*), 1.01 (d, 3H, *i-Bu-CH_3*), 0.83 (d, 3H, *i-Bu-CH_3*), 0.77 (d, 3H, *i-Bu-CH_3*). $^{13}C\{^1H\}$ NMR (126 MHz, C_6D_6): δ 180.1 (d, $^1J_{Rh-C} = 61.2$ Hz), 171.6, 170.1, 142.0 (br d, *ipso-C*), 134.6, 133.2, 133.1, 130.8, 130.7, 75.1, 73.6, 66.3, 64.5, 43.4, 42.8, 33.6, 33.1, 26.3, 25.5, 24.2, 24.1, 22.6, 21.4, 21.3, 21.2. EI-MS (m/z): 556 $[M - CO]^+$, 520 $[M - CO - HCl]^+$, 484 $[M - CO - 2HCl]^+$.

[RhCl₂{(S,S)-ib-benbox(Me₂)}(t-BuNC)] (6d). To an orange solution of $[RhCl_2\{(S,S)\text{-ib-benbox(Me}_2)\}]$ (4d) (55.7 mg, 0.10 mmol) in methylene chloride (10 mL) at ambient temperature was added *t*-BuNC (8.3 mg, 0.10 mmol), producing an immediate yellow suspension. After stirring overnight the mixture was filtered. A yellow microcrystalline solid was obtained after removing the solvent. The compound was purified by column chromatography with methylene chloride as eluent. Yield: 52.5 mg, 82%. Mp: >260 °C. Anal. Calcd for $C_{29}H_{44}Cl_2N_3O_2Rh$: C, 54.38; H, 6.92; N, 6.56. Found: C, 54.10; H, 6.98; N, 6.28. IR (KBr, cm^{-1}): 2177, 1669 (ν_{CN}). 1H NMR (300 MHz, C_6D_6): δ 6.76 (s, 1H, *CH*), 5.0–4.3 (br, 4H), 4.41 (m, 2H), 3.82 (m, 2H), 3.64 (t, 2H), 2.64 (br, 2H, *i-Bu-CH*), 2.16 (s, 6H, CH_3), 1.37 (m, 2H, *i-Bu-CH_2*), 1.30 (m, 2H, *i-Bu-CH_2*), 1.21 (s, 9H, *t*-BuNC- CH_3), 0.86 (d, 6H, *i-Bu-CH_3*), 0.72 (d, 6H, *i-Bu-CH_3*). EI-MS (m/z): 556 $[M - t\text{-BuNC}]^+$, 520 $[M - t\text{-BuNC} - HCl]^+$, 484 $[M - t\text{-BuNC} - 2HCl]^+$.

General Procedure for Synthesis of Rhodium Complexes 7c and 8c. A 2.0 M solution of dimethylzinc in toluene (0.5 mL, 1.0 mmol) was added dropwise at –30 °C to an orange solution of $[RhCl_2\{(S,S)\text{-ip-benbox}\}]$ (3c) (250 mg, 0.5 mmol) or $[RhCl_2\{(S,S)\text{-ip-benbox(Me}_2)\}]$ (4c) (265 mg, 0.5 mmol) in 10 mL of tetrahydrofuran. The mixture was warmed to room temperature and was then stirred for 2 h, giving a yellow cloudy solution. The solution was concentrated to dryness in vacuo. The yellow-brown residue was dissolved in methylene chloride (10 mL), and 1 g of alumina(III) was added. After stirring for 2 h, the bright yellow suspension was filtered and

the alumina was washed with methylene chloride (2 \times 5 mL). A bright yellow microcrystalline solid was obtained after the solvent had been removed from the filtrate under vacuum.

[RhMe(Cl){(S,S)-ip-benbox}] (7c): yield 89 mg, 37%. Mp: 92–94 °C (dec). Anal. Calcd for $C_{21}H_{30}ClN_2O_2Rh$: C, 52.45; H, 6.29; N, 5.83. Found: C, 52.21; H, 6.51; N, 5.47. IR (KBr, cm^{-1}): 1673 (ν_{CN}). 1H NMR (300 MHz, C_6D_6): δ 6.79 (t, 1H, *CH*), 6.61 (t, 2H, *CH*), 5.12 (m, 2H), 3.95 (m, 2H), 3.72–3.55 (m, 4H), 3.45 (d, 2H, CH_2 , $^2J_{H-H} = 16.8$ Hz), 3.32 (d, 1H, CH_2 , $^2J_{H-H} = 18.8$ Hz), 2.06 (sept, 1H, *i-Pr-CH*), 1.89 (sept, 1H, *i-Pr-CH*), 1.16 (d, 3H, $Rh-CH_3$, $^2J_{Rh-H} = 2.0$ Hz), 0.82 (d, 3H, CH_3), 0.76 (d, 3H, CH_3), 0.72 (d, 3H, CH_3), 0.66 (d, 3H, CH_3). $^{13}C\{^1H\}$ NMR (126 MHz, C_6D_6): δ 169.8, 168.8, 146.6 (d, $^1J_{Rh-C} = 41.6$ Hz), 139.3, 138.8, 127.0, 126.7, 123.0, 71.0, 70.6, 69.9, 69.4, 37.6, 36.2, 31.6, 30.5, 19.9, 19.6, 17.1, 16.4, –5.6 (d, $^1J_{Rh-C} = 28.0$ Hz).

[RhMe(Cl){(S,S)-ip-benbox(Me₂)}] (8c): yield 91 mg, 36%. Mp: 136–140 °C (dec). Anal. Calcd for $C_{23}H_{34}ClN_2O_2Rh$: C, 54.29; H, 6.73; N, 5.50. Found: C, 54.36; H, 6.65; N, 5.18. IR (KBr, cm^{-1}): 1672 (ν_{CN}). 1H NMR (300 MHz, C_6D_6): δ 6.54 (s, 1H, *CH*), 5.17 (m, 2H), 3.90 (m, 1H, *ox-CH*), 3.81–3.50 (m, 7H), 2.09 (sept, 1H, *i-Pr-CH*), 2.00 (s, 3H, CH_3), 1.99 (s, 3H, CH_3), 1.88 (sept, 1H, *i-Pr-CH*), 1.18 (d, 3H, $Rh-CH_3$, $^2J_{Rh-H} = 2.0$ Hz), 0.88 (d, 3H, *i-Pr-CH_3*), 0.80 (d, 3H, *i-Pr-CH_3*), 0.74 (d, 3H, *i-Pr-CH_3*), 0.72 (d, 3H, *i-Pr-CH_3*). $^{13}C\{^1H\}$ NMR (126 MHz, C_6D_6): δ 170.2, 168.5, 145.7 (d, $^1J_{Rh-C} = 43.6$ Hz), 135.3, 135.0, 132.3, 132.1, 128.5, 71.0, 70.5, 69.2, 67.8, 32.3, 31.7, 31.6, 30.7, 21.2, 21.1, 19.9, 19.7, 17.2, 16.5, –5.5 (d, $^1J_{Rh-C} = 28.7$ Hz). EIMS (m/z): 508 $[M]^+$, 472 $[M - HCl]^+$, 370 $[M - HCl - Rh]^+$.

General Procedure for Synthesis of Rhodium Complexes 9c and 10c. To a yellow methylene chloride (5 mL) solution of $[RhMe(Cl)\{(S,S)\text{-ip-benbox}\}]$ (7c) (48 mg, 0.10 mmol) or $[RhMe(Cl)\{(S,S)\text{-ip-benbox(Me}_2)\}]$ (8c) (51 mg, 0.10 mmol) was added AgOTf (25.7 mg, 0.10 mmol), producing a yellow suspension. After stirring overnight, the bright orange-yellow suspension was filtered. The methylene chloride was removed under vacuum, leaving a yellow microcrystalline solid. Crystals suitable for X-ray diffraction were obtained by layering a concentrated methylene chloride solution of 9c with pentane.

[RhMe(OTf){(S,S)-ip-benbox}] (9c): yield 55 mg, 93%. Mp: 128–132 °C (dec). Anal. Calcd for $C_{22}H_{30}F_3N_2O_5RhS$: C, 44.45; H, 5.09; N, 4.71. Found: C, 44.51; H, 5.11; N, 4.67. IR (KBr, cm^{-1}): 1669 (ν_{CN}). 1H NMR (300 MHz, C_6D_6): δ 6.74 (t, 1H, *CH*), 6.53 (d, 1H, *CH*), 6.49 (d, 1H, *CH*), 4.68 (m, 1H, *ox-CH*), 4.58 (d, 1H, CH_2 , $^2J_{H-H} = 18.4$ Hz), 3.73–3.62 (m, 6H), 3.48 (d, 1H, CH_2 , $^2J_{H-H} = 18.4$ Hz), 3.32 (d, 1H, CH_2 , $^2J_{H-H} = 19.2$ Hz), 2.14 (sept, 1H, *i-Pr-CH*), 1.91 (sept, 1H, *i-Pr-CH*), 1.07 (d, 3H, $Rh-CH_3$, $^2J_{Rh-H} = 2.4$ Hz), 0.72 (d, 3H, CH_3), 0.68 (d, 3H, CH_3), 0.55 (d, 3H, CH_3), 0.53 (d, 3H, CH_3). $^{13}C\{^1H\}$ NMR (126 MHz, C_6D_6): δ 170.5, 170.3 (d, $^2J_{Rh-C} = 1.7$ Hz), 141.2 (d, $^1J_{Rh-C} = 45.6$ Hz), 139.0 (d, $^2J_{Rh-C} = 2.0$ Hz), 138.8, 128.3, 127.3, 123.9, 71.1, 70.3, 70.2, 69.7, 36.5 (d, $^3J_{Rh-C} = 1.4$ Hz), 36.1 (d, $^3J_{Rh-C} = 1.4$ Hz), 31.5, 29.7, 22.2, 19.2, 16.7, 14.9, –8.3 (d, $^1J_{Rh-C} = 31.6$ Hz); the $^{13}C\{^1H\}$ NMR resonance of the triflate ligand was not observed. ^{19}F NMR (376.1 MHz, C_6D_6): δ –77.7. EIMS (m/z): 594 $[M]^+$, 579 $[M - CH_3]^+$, 444 $[M - HOTf]^+$.

[RhMe(OTf){(S,S)-ip-benbox(Me₂)}] (10c): yield 59 mg, 95%. Mp: 108–110 °C (dec). Anal. Calcd for $C_{24}H_{34}F_3N_2O_5RhS$: C, 46.31; H, 5.51; N, 4.50. Found: C, 46.54; H, 5.24; N, 4.23. IR (KBr, cm^{-1}): 1678 (ν_{CN}). 1H NMR (300 MHz, C_6D_6): δ 6.49 (s, 1H, *CH*), 4.76 (m, 1H, *ox-CH*), 4.56 (d, 1H, CH_2 , $^2J_{H-H} = 18.0$ Hz), 3.81–3.55 (m, 7H), 3.44 (d, 1H, CH_2 , $^2J_{H-H} = 18.8$ Hz), 2.21 (sept, 1H, *i-Pr-CH*), 1.99 (sept, 1H, *i-Pr-CH*), 1.92 (s, 3H, CH_3), 1.89 (s, 3H, CH_3), 1.13 (d, 3H, $Rh-CH_3$, $^2J_{Rh-H} = 2.8$ Hz), 0.75 (d, 3H, *i-Pr-CH_3*), 0.72 (d, 3H, *i-Pr-CH_3*), 0.61 (d, 3H, *i-Pr-CH_3*), 0.55 (d, 3H, *i-Pr-CH_3*). $^{13}C\{^1H\}$ NMR (126 MHz, C_6D_6): δ 171.0, 170.2, 141.6 (d, $^1J_{Rh-C} = 45.0$ Hz), 135.1 (d, $^2J_{Rh-C} = 1.6$ Hz), 134.8, 133.1, 132.9, 129.5, 72.4, 70.2 (2 \times),

69.8, 32.0, 31.4 (2 \times), 29.9, 22.8, 21.1, 20.9, 19.4, 17.0, 15.1, -8.0 (d, $^1J_{\text{Rh-C}} = 30.0$ Hz); the $^{13}\text{C}\{^1\text{H}\}$ NMR resonance of the triflate ligand was not observed. ^{19}F NMR (376.1 MHz, C_6D_6): $\delta -77.7$. EIMS (m/z): 622 $[\text{M}]^+$, 607 $[\text{M} - \text{CH}_3]^+$, 472 $[\text{M} - \text{HOTf}]^+$.

[RhMe{(S,S)-ip-benbox(Me₂)}][BARf] (11c). A yellow solution of $[\text{RhMe}(\text{OTf})\{(S,S)\text{-ip-benbox}(\text{Me}_2)\}]$ (**10c**) (62.3 mg, 0.10 mmol) in methylene chloride (10 mL) was prepared. NaBARf (88.6 mg, 0.10 mmol) was added at ambient temperature, producing a cloudy yellow mixture. After stirring for 4 h at room temperature, the mixture was filtered and the solvent was removed under vacuum. The resulting oil was triturated with pentane (3 \times 5 mL), and a yellow microcrystalline solid was obtained after the residual solvent was removed under vacuum. Yield: 138 mg, 97%. Mp: 72–74 °C (dec). Anal. Calcd for $\text{C}_{55}\text{H}_{46}\text{F}_{24}\text{N}_2\text{O}_2\text{RhB}$: C, 49.42; H, 3.47; N, 2.10. Found: C, 49.72; H, 3.47; N, 2.00. IR (KBr, cm^{-1}): 2809 (ν_{CH}), 1678, 1610 (ν_{CN}). ^1H NMR (300 MHz, CD_2Cl_2): δ 7.74 (s, 8H, BARf-CH), 7.58 (s, 4H, BARf-CH), 6.83 (s, 1H, CH), 4.60 (t, 1H, ox-CH₂), 4.44 (dd, 1H, ox-CH₂), 4.39 (t, 1H, ox-CH₂), 4.34 (t, 1H, ox-CH₂), 4.05 (m, 2H, ox-CH), 4.00 (d, 1H, CH₂, $^2J_{\text{H-H}} = 18.8$ Hz), 3.92 (s, 2H, CH₂), 3.88 (d, 1H, CH₂, $^2J_{\text{H-H}} = 18.8$ Hz), 2.26 (s, 3H, CH₃), 2.25 (s, 3H, CH₃), 1.94 (sept, 1H, *i*-Pr-CH), 1.89 (sept, 1H, *i*-Pr-CH), 1.32 (d, 3H, Rh-CH₃, $^2J_{\text{Rh-H}} = 2.0$ Hz), 0.91 (d, 6H, *i*-Pr-CH₃), 0.89 (d, 3H, *i*-Pr-CH₃), 0.82 (d, 3H, *i*-Pr-CH₃). $^{13}\text{C}\{^1\text{H}\}$ NMR (126 MHz, CD_2Cl_2): δ 172.0 (d, $^2J_{\text{Rh-C}} = 2.3$ Hz), 171.4, 162.4 (q, $^1J_{\text{B-C}} = 50$ Hz, *ipso*-C-BARf), 139.1 (d, $^1J_{\text{Rh-C}} = 40.1$ Hz), 137.6, 135.4 (s, *o*-C-BARf), 135.2, 135.1 (d, $^2J_{\text{Rh-C}} = 2.0$ Hz), 134.2 (d, $^2J_{\text{Rh-C}} = 2.0$ Hz), 131.3, 129.5 (qq, $^2J_{\text{F-C}} = 31$ Hz, $^4J_{\text{F-C}} = 3$ Hz, *m*-C-BARf), 125.2 (q, $^1J_{\text{F-C}} = 270$ Hz, BARfCF₃), 118.1 (sept, $^3J_{\text{F-C}} = 4$ Hz), 72.7, 72.5, 72.3, 70.4, 32.3, 32.2 (d, $^3J_{\text{Rh-C}} = 2.1$ Hz), 31.9 (d, $^3J_{\text{Rh-C}} = 1.4$ Hz), 31.8, 21.8, 21.7, 21.6 (2 \times), 16.9, 16.8, -3.3 (d, $^1J_{\text{Rh-C}} = 32.7$ Hz). ^{19}F NMR (376.1 MHz, CD_2Cl_2): $\delta -61.0$. FABMS (m/z): 473 $[\text{M} - \text{BARf}]^+$, 458 $[\text{M} - \text{BARf} - \text{CH}_3]^+$.

[Rh(C₂H₄){(S,S)-ip-benbox(Me₂)(2-Me)}][BARf](12c). In the glovebox, a Teflon-stoppered sealable 50 mL reaction vessel was charged with **11c** (70.0 mg, 0.052 mmol) and 5 mL of CH_2Cl_2 . The solution was degassed with three freeze–pump–thaw cycles, then exposed to approximately 700 mbar of ethylene. After 14 h at room temperature, the volatile materials were removed under vacuum. The resulting yellow oil was triturated with pentane (3 \times 3 mL), and a yellow microcrystalline solid was obtained after the residual solvent had been removed under vacuum. Yield: 69.3 mg, 97%. Anal. Calcd for $\text{C}_{57}\text{H}_{50}\text{F}_{24}\text{N}_2\text{O}_2\text{RhB}$: C, 50.16; H, 3.69; N, 2.05. Found: C, 50.04; H, 3.69; N, 1.89. IR (CD_2Cl_2 , cm^{-1}): 1609 (ν_{CN}). ^1H NMR (300 MHz, CD_2Cl_2): δ 7.72 (s, 8H, BARf-CH), 7.56 (s, 4H, BARf-CH), 7.31 (s, 1H, CH), 4.25 (m, 2H, ox-CH), 4.15 (t, 1H, ox-CH₂), 4.08 (t, 1H, ox-CH₂), 3.92–3.81 (m, 6H), 3.50 (m, 2H, C₂H₄), 3.27 (m, 2H, C₂H₄), 2.72 (s, 3H, CH₃), 2.37 (s, 3H, CH₃), 2.31 (s, 3H, CH₃), 2.04 (m, 1H, *i*-Pr-CH), 1.41 (m, 1H, *i*-Pr-CH), 0.86 (d, 3H, *i*-Pr-CH₃), 0.75 (d, 3H, *i*-Pr-CH₃), 0.73 (d, 3H, *i*-Pr-CH₃), 0.48 (d, 3H, *i*-Pr-CH₃). $^{13}\text{C}\{^1\text{H}\}$ NMR (100 MHz, CD_2Cl_2): δ 177.1, 175.1, 163.5 (q, $^1J_{\text{B-C}} = 49$ Hz, *ipso*-C-BARf), 138.5, 138.4, 137.8, 136.6 (s, *o*-C-BARf), 135.1 (2 \times), 134.4, 130.8 (qq, $^2J_{\text{F-C}} = 30$ Hz, $^4J_{\text{F-C}} = 3$ Hz, *m*-C-BARf), 126.4 (q, $^1J_{\text{F-C}} = 271$ Hz, BARfCF₃), 119.3 (sept, $^3J_{\text{F-C}} = 4$ Hz), 71.6, 70.9, 70.3, 69.9, 32.5, 31.2, 30.6, 30.3, 24.1, 22.0, 21.7, 20.6, 20.1, 15.9, 15.3. No carbon peaks for the bound ethylene ligand were observed. ^{19}F NMR (376.1 MHz, CD_2Cl_2): $\delta -61.0$.

[Rh(CO){(S,S)-ip-benbox(Me₂)(2-Me)}][BARf] (13c). In the glovebox, a J-Young NMR tube was charged with complex **11c** (7.0 mg, 0.005 mmol) and 300 μL of CD_2Cl_2 . The solution was degassed with three freeze–pump–thaw cycles, and the tube was exposed to 700 mbar of CO. The reaction progress was monitored by ^1H NMR spectroscopy. ^1H NMR after 10 min revealed the formation of **13c**, which is fully converted to **14c** within 14 h and could not be isolated independently. ^1H NMR (300 MHz, CD_2Cl_2): δ 7.72 (s, 8H, BARf-CH), 7.56 (s, 4H, BARf-

CH), 7.15 (s, 1H, CH), 4.44 (m, 4H, ox-CH₂), 4.17 (d, 1H, CH₂, $^2J_{\text{H-H}} = 17.2$ Hz), 4.06 (d, 1H, CH₂, $^2J_{\text{H-H}} = 18.8$ Hz), 3.92 (d, 1H, CH₂, $^2J_{\text{H-H}} = 5.2$ Hz), 3.89 (d, 1H, CH₂, $^2J_{\text{H-H}} = 2.8$ Hz), 3.70 (m, 1H, ox-CH), 3.59 (m, 1H, ox-CH), 2.86 (s, 3H, CH₃), 2.32 (m, 1H, *i*-Pr-CH), 2.28 (m, 1H, *i*-Pr-CH), 2.21 (s, 3H, CH₃), 2.19 (s, 3H, CH₃), 0.91 (d, 3H, *i*-Pr-CH₃), 0.86 (d, 3H, *i*-Pr-CH₃), 0.71 (d, 3H, *i*-Pr-CH₃), 0.56 (d, 3H, *i*-Pr-CH₃). ^{19}F NMR (376.1 MHz, CD_2Cl_2): $\delta -61.0$.

[Rh(CO)₂{(S,S)-ip-benbox(Me₂)(2-Me)}][BARf] (14c). In the glovebox, a Teflon-stoppered sealable 50 mL reaction vessel was charged with **11c** (55.2 mg, 0.041 mmol) and 10 mL of CH_2Cl_2 . The solution was degassed with three freeze–pump–thaw cycles, then exposed to approximately 700 mbar of CO, and after 14 h at room temperature the volatile materials were removed under vacuum. A yellow microcrystalline solid was isolated. The same procedure was used to synthesize the ^{13}C -enriched isomer with isotopically enriched ^{13}C for identification of the IR bands and ^{13}C NMR shifts. Yield: 54.0 mg, 96%. Anal. Calcd for $\text{C}_{57}\text{H}_{46}\text{F}_{24}\text{N}_2\text{O}_4\text{RhB}$: C, 49.15; H, 3.33; N, 2.01. Found: C, 49.55; H, 3.51; N, 1.71. IR (KBr): 2094, 2029 ($\nu_{12\text{CO}}$), 2052, 1993 ($\nu_{13\text{CO}}$), 1614 (ν_{CN}). ^1H NMR (300 MHz, CD_2Cl_2): δ 7.72 (s, 8H, BARf-CH), 7.56 (s, 4H, BARf-CH), 7.24 (s, 1H, CH), 4.60–4.35 (m, 4H), 4.11–3.84 (m, 6H), 2.43 (s, 3H, CH₃), 2.40 (s, 3H, CH₃), 2.15 (m, 2H, *i*-Pr-CH), 1.91 (s, 3H, CH₃), 0.96 (d, 3H, *i*-Pr-CH₃), 0.91 (d, 3H, *i*-Pr-CH₃), 0.83 (d, 3H, *i*-Pr-CH₃), 0.80 (d, 3H, *i*-Pr-CH₃). $^{13}\text{C}\{^1\text{H}\}$ NMR (125 MHz, CD_2Cl_2): δ 180.3 (identified only in ^{13}C -enriched spectrum, dd, $^2J_{\text{C-C}} = 6.3$ Hz, $^1J_{\text{Rh-C}} = 70$ Hz), 179.7 (identified only in ^{13}C -enriched spectrum, dd, $^2J_{\text{C-C}} = 6.3$ Hz, $^1J_{\text{Rh-C}} = 70$ Hz), 176.7, 176.5, 163.6 (q, $^1J_{\text{B-C}} = 50$ Hz, *ipso*-C-BARf), 133.5 (s, *o*-C-BARf), 131.4, 131.2 (2 \times), 130.8 (qq, $^2J_{\text{F-C}} = 30$ Hz, $^4J_{\text{F-C}} = 3$ Hz, *m*-C-BARf), 129.4 (2 \times), 129.2, 126.3 (q, $^1J_{\text{F-C}} = 271$ Hz, BARfCF₃), 119.3 (sept, $^3J_{\text{F-C}} = 4$ Hz), 74.6, 72.3, 70.8, 70.6, 32.3, 32.1, 31.5, 31.3, 21.6, 21.5, 20.9, 20.8, 19.4, 16.5, 15.1. ^{19}F NMR (376.1 MHz, CD_2Cl_2): $\delta -61.0$.

General Procedure for the Preparation of Rhodium-(II) Complexes 15. $\text{RhCl}_3 \cdot 3\text{H}_2\text{O}$ (263 mg, 1.0 mmol) was added to a solution of the bisoxazoline **2e** (500 mg, 1.3 mmol) or **2g** (426 mg, 1.3 mmol), in 10 mL of degassed ethanol at 70 °C. The resulting orange-red suspension was heated at reflux for 30 min. After evaporation to dryness at room temperature, column chromatography on silica was performed with methylene chloride as eluent, giving as the first fraction (orange) the corresponding rhodium(III) complex. The second fraction (yellow) yielded the rhodium(II) complex as an air-stable yellow microcrystalline solid. The yield of the *tert*-butyl-substituted complex **15e** was dramatically increased by running the reaction at higher dilution (quantities listed above in 100 mL of ethanol). Crystals suitable for elemental and X-ray analysis were obtained by layering a concentrated benzene solution of **15g** with pentane.

[RhCl₂{(S,S)-tb-benbox(Me₂)}(H)] (15e): yield 106 mg, 19% (reaction run in 10 mL ethanol); 318 mg, 57% (reaction run in 100 mL ethanol). Mp: ca. 180 °C. $R_f = 0.31$ (methylene chloride). Anal. Calcd for $\text{C}_{24}\text{H}_{36}\text{Cl}_2\text{N}_2\text{O}_2\text{Rh}$: C, 51.63; H, 6.50; N, 5.02. Found: C, 51.97; H, 6.54; N, 4.82. IR (KBr, cm^{-1}): 1647, 1637 (ν_{CN}). ^1H NMR (300 MHz, C_6D_6): δ 20.5, 18.6, 11.1, 8.5, -37.7. FABMS (m/z): 522.3 $[\text{M} - \text{Cl}]^+$, 486.3 $[\text{M} - \text{Cl} - \text{HCl}]^+$. $\mu_{\text{eff}} = 1.87 \mu_{\text{B}}$ (solution).

[RhCl₂{dm-benbox(Me₂)}(H)] (15g): yield 246 mg, 49%. Mp: 190–192 °C. $R_f = 0.06$ (methylene chloride). Anal. Calcd for $\text{C}_{20}\text{H}_{28}\text{Cl}_2\text{N}_2\text{O}_2\text{Rh}$: C 47.83; H 5.62; N 5.58. Found: C 47.76; H 5.90; N 5.44. IR (KBr, cm^{-1}): 1654, 1641 (ν_{CN}). ^1H NMR (300 MHz, C_6D_6): δ 35.8, 20.6, 17.5, 10.9, -33.3. EIMS (m/z): 465 $[\text{M} - \text{HCl}]^+$, 429 $[\text{M} - \text{Cl} - \text{HCl}]^+$. $\mu_{\text{eff}} = 1.98 \mu_{\text{B}}$ (solution), $\mu_{\text{eff}} = 2.00(2) \mu_{\text{B}}$ (solid state).

Thermolysis of 15g. The rhodium(II) complex **15g** (13 mg, 0.026 mmol) and 1,4-dimethoxybenzene (standard, 2.7 mg, 0.019 mmol) were dissolved in 300 μL of C_6D_6 and transferred to a medium-walled NMR tube. The solution was degassed, and the tube was flame-sealed under vacuum. The sample was

warmed to room temperature, and an initial ^1H NMR spectrum was recorded. The tube was heated at $75\text{ }^\circ\text{C}$ in an oil bath and cooled to room temperature, and a ^1H NMR spectrum was recorded. The progress of the reaction was analyzed by integrating the product signals against the internal standard. After 48 h of heating at $75\text{ }^\circ\text{C}$, formation of **4g** (42%) and **16g** (39%) was observed. The formation of a small amount of rhodium metal at the NMR tube surface was also observed.

[RhCl₂(H){(*S,S*)-dm-benbox(Me₂)H}] (16g). A high-pressure steel reaction vessel was charged with a dark orange solution of the rhodium complex **4g** (121 mg, 0.24 mmol) in 30 mL of benzene. The vessel was pressurized to 35 atm with H₂ and heated to $75\text{ }^\circ\text{C}$ for 10 h. After this time, the pressure was vented, and the resulting yellow solution was filtered, pumped down, and then triturated with pentane ($3 \times 7\text{ mL}$) to yield a spectroscopically and analytically pure yellow powder. Yield = 94 mg, 75%. Anal. Calcd for C₂₀H₂₉Cl₂N₂O₂-Rh: C, 47.73; H, 5.81; N, 5.57. Found: C, 47.61; H, 5.85; N, 5.51. IR (KBr): 2197 (ν_{RhH}), 1642 (ν_{CN}). ^1H NMR (300 MHz, C₆D₆): δ 9.03 (d, 1H, CH, $^2J_{\text{H-H}} = 3.3\text{ Hz}$), 7.18 (s, 1H, CH), 3.69 (d, 2H, CH₂, $^2J_{\text{H-H}} = 16.6\text{ Hz}$), 3.46 (m, 6H, ox-CH₂, CH₂), 2.01 (s, 6H, CH₃), 1.49 (s, 6H, ox-CH₃), 1.28 (s, 6H, ox-CH₃), -19.70 (dd, 1H, Rh-H, $J_{\text{H-H}} = 3.3\text{ Hz}$, $^1J_{\text{Rh-H}} = 18.8\text{ Hz}$). ^{13}C - $\{^1\text{H}\}$ NMR (126 MHz, CDCl₃): δ 170.7, 136.6, 134.1, 130.5, 121.6, 79.1, 70.0, 31.4, 29.1, 29.0, 18.7.

X-ray Structure Determinations. General Considerations. X-ray crystal structures were obtained by Fred Hollander, Dana Caulder, and Allan Oliver at the UCB X-ray facility (CHEXRAY). Crystals were mounted on glass fibers using Paratone N hydrocarbon oil. All measurements were made on a SMART³⁰ CCD area detector with graphite-monochromated Mo K α radiation ($\lambda = 0.71069\text{ \AA}$). The data were collected with a detector position of 60.00 mm. Data were integrated by the program SAINT³¹ and were corrected for Lorentz and polarization effects. Data were analyzed for agreement and possible absorption using XPREP.³² The structures were solved by direct methods³³ and expanded using Fourier techniques.³⁴

(a) [RhCl₂{(*S,S*)-ip-benbox(Me₂)}] (4c). One molecule of

(30) SMART: Area-Detector Software Package; Siemens Industrial Automation Inc.: Madison, WI, 1995.

(31) SAINT: SAX Area-Detector Integration Program, V4.024; Siemens Industrial Automation Inc.: Madison, WI, 1995.

(32) XPREP: (v. 5.03) Part of the SHELXTL Crystal Structure Determination; Siemens Industrial Automation Inc.: Madison, WI, 1995.

(33) SIR92: Altomare, A.; Cascarano, M.; Giacovazzo, C.; Guagliardi, A. *J. Appl. Crystallogr.* **1993**, *26*, 343.

(34) DIRDIF94: Beurskens, P. T.; Admiraal, G.; Beurskens, G.; Bosman, W. P.; de Gelder, R.; Israel, R.; Smits, J. M. M. The DIRDIF-94 program system, Technical Report of the Crystallography Laboratory; University of Nijmegen: The Netherlands, 1994.

CH₂Cl₂ cocrystallized with **4c**. The data were collected using 10 s frames with an ω scan of 0.3° . Empirical absorption corrections based on comparison of redundant and equivalent reflections were applied using SADABS³⁵ ($T_{\text{max}} = 0.93$, $T_{\text{min}} = 0.72$). The maximum peak in the final difference map was $0.81\text{ e}^-/\text{\AA}^3$, and the minimum peak was $-0.47\text{ e}^-/\text{\AA}^3$. The correct enantiomorphs of the molecule and space group were determined by comparison of Friedel pairs.

(b) [RhMe(OTf){(*S,S*)-ip-benbox}] (9c). The compound crystallizes with four molecules in the asymmetric unit of the acentric space group *P2*₁. The data were collected using 20 s frames with an ω scan of 0.3° . Empirical absorption corrections based on comparison of redundant and equivalent reflections were applied using SADABS³⁵ ($T_{\text{max}} = 0.98$, $T_{\text{min}} = 0.60$). The maximum peak in the final difference map was $1.21\text{ e}^-/\text{\AA}^3$, and the minimum peak was $-1.74\text{ e}^-/\text{\AA}^3$. The correct enantiomorphs of the molecule and space group were determined by comparison of Friedel pairs.

(c) [RhCl₂{dm-benbox(Me₂)H}] (15g). The data were collected using 10 s frames with an ω scan of 0.3° . Empirical absorption corrections based on comparison of redundant and equivalent reflections were applied using SADABS³⁵ ($T_{\text{max}} = 0.90$, $T_{\text{min}} = 0.71$). The maximum peak in the final difference map was $0.44\text{ e}^-/\text{\AA}^3$, and the minimum peak was $-0.71\text{ e}^-/\text{\AA}^3$.

Acknowledgment. Drs. Fred Hollander, Dana Caulder, and Allan Oliver at the UCB X-ray diffraction facility (CHEXRAY) are gratefully acknowledged for determination of the crystal structures of **4c**, **9c**, and **15g**. This work was carried out under the auspices of a CRADA project, administered by the Lawrence Berkeley National Laboratory under contract no. DE-AC03-76SF00098, in cooperation with the E. I. DuPont Co, and funded under the Initiatives for Proliferation Prevention Program of the U.S. Department of Energy. The Center for New Directions in Organic Synthesis is supported by Bristol-Myers Squibb as Sponsoring Member. M.G. thanks Deutsche Forschungsgemeinschaft for a Postdoctoral Fellowship. J.R.K. thanks the National Science Foundation for a Predoctoral Fellowship.

Supporting Information Available: Spectral and analytical data for compounds **1b-g**, **2b-g**, **3d-g**, and **4e-g**; crystal structure data for **4c**, **9c**, and **15g**, including additional molecular structure diagrams, tables of positional and thermal parameters, bond distances and angles.

OM0207562

(35) SADABS: Siemens Area Detector Absorption Correction Program; Sheldrick, G. 1996. Advance copy, private communication.